Silent News in China's Monetary Policy Announcements: Dual-Shock Identification with Ordered Heteroskedasticity

Mucai Lin* Zhiwu Hong† Linlin Niu‡

January 24, 2026

Abstract

China's monetary policy employs a dual-target framework, where announcements explicitly adjust one target while silently signaling the other. Existing single-shock models ignore this embedded dual-shock structure. We propose identification via ordered heteroskedasticity: loud-news shocks exhibit higher variance than silent-news shocks. Applied to Chinese Treasury yields, our model outperforms single-shock specifications. Silent news—particularly price signals within quantity announcements—provides potent forward guidance that predicts future policy adjustments. Both news types trigger significant and persistent responses in yields and money-market rates. These findings highlight the role of silent news in central bank communication and deepen understanding of China's dual-target policy transmission.

JEL Classification: E43; E52; E58

Keywords: Monetary Policy Announcements; Silent News; Heteroskedasticity; Dual-Shock Identification.

*The Digital Fujian "Belt and Road" Service Industry Big Data Research Institute at Huaqiao University, China; Institute of Quantitative Economics and Statistics, Huaqiao University, China.

†Business School, China University of Political Science and Law, China. Corresponding author: Room B406, Administrative Building, China University of Political Science and Law, Beijing 102249, China. E-mail: CU212049@cupl.edu.cn. Tel: +86 18612933426.

‡Center for Macroeconomic Research at Xiamen University, China; Wang Yanan Institute for Studies in Economics (WISE), Xiamen University, China.

1 Introduction

As the world's second-largest economy, China's monetary policy profoundly influences global financial conditions. Unlike advanced economies that rely primarily on price-target-based frameworks, China's central bank, the People's Bank of China (PBoC), employs a dual-target framework, coordinating quantity-target-based tools (e.g., Reserve Requirement Ratio, RRR) with price-target-based tools (e.g., Benchmark Lending and Deposit Rates or Medium-term Lending Facility rate, BLDR or MLF rate). As Figure 1 shows, these tools have historically co-moved, reflecting strategic coordination. A key operational practice, however, is that the PBoC typically adjusts only one tool at a time, with simultaneous adjustments being rare (11% of events; see Appendix Table A.1). This practice implies that a single announcement, while explicitly changing one target, may implicitly signals future intentions for the other.

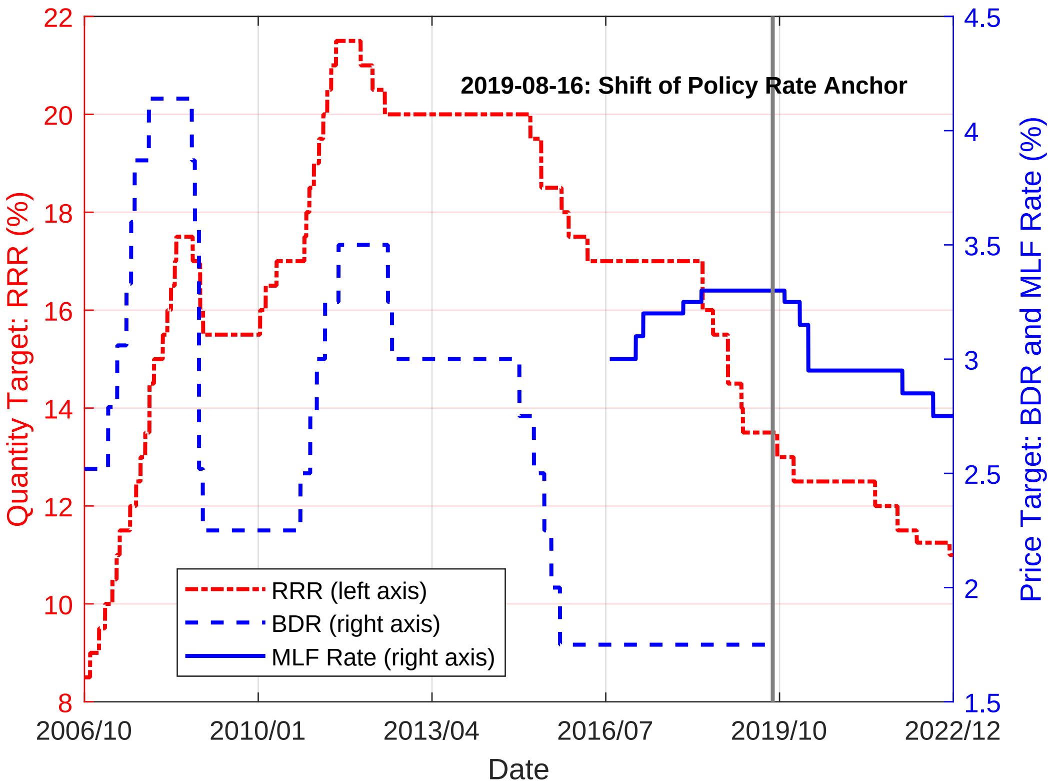

Figure 1: Co-movement of China's Monetary Policy Tools

Note: This figure plots the time series of China's Reserve Requirement Ratio (RRR) for large deposit-taking financial institutions, the 1-year Benchmark Deposit Rate (BDR), and the 1-year Medium-term Lending Facility (MLF) rate from October 8, 2006, to December 31, 2022. The vertical line marks August 16, 2019, when the PBoC shifted its primary policy rate anchor. The co-movement of these series demonstrates the operational coordination between quantity-target-based and price-target-based tools within China's dual-target monetary policy framework.

Market reactions provide clear evidence that China's policy announcements contain dual signals. A case in point is the PBoC's quantity-target-based announcement on June 7, 2008, when it raised the RRR. Subsequent market commentary (*China Securities Journal, June 10, 2008*) immediately inferred implications for the price tool, stating: "*the likelihood of an interest rate increase this month has decreased... [but] the probability of China raising interest rates in the second half of the year continues to rise.*"[1] This demonstrates that while the PBoC loudly announced a quantity adjustment, the announcement also embedded potent silent news about future price targets. We therefore refer to the explicit, announced signal as loud news and the implicit, inferred signal as silent news.

A rich literature, established primarily in the context of the U.S. Federal Reserve, demonstrates that monetary policy announcements contain multidimensional information, triggering more than one type of shock (Gürkaynak et al., 2005). The multidimensionality has been shown to arise from either the information structure of announcements or the use of multiple policy tools. However, despite China's explicit dual-tool framework, existing studies on PBoC announcements have almost uniformly treated policy shocks as single-dimensional (Lin and Niu, 2021; Das and Song, 2023; He et al., 2023; Lu et al., 2023). This critical oversight likely reflects two misconceptions: first, the tendency of PBoC announcements to adjust only one tool at a time has led researchers to assume a single associated shock; second, the perceived textual brevity of PBoC statements, which lack the detailed forward guidance of FOMC communications, has been mistakenly interpreted as a lack of additional "silent" information (Appendix A.1 provides two examples of PBoC statements).

A central challenge in identifying these dual shocks in China lies in the absence of suitable financial derivatives. Unlike the U.S., which has federal funds futures to directly measure market expectations of the policy target, China lacks analogous assets (e.g., RRR futures or reliable policy rate futures). This data constraint renders conventional identification strategies, which rely on observable target surprises (Kuttner, 2001; Gürkaynak et al., 2005), inapplicable. Alternative strategies that treat the target shock as unobservable and impose economic theory-based constraints to isolate shock dimensions (Cieslak and Schrimpf, 2019; Jarociński and Karadi, 2020) are also challenging. Sufficient economic knowledge to distinguish between quantity and price targets is not readily available due to the uniqueness of China's monetary policy framework.

To address this challenge, we develop an innovative identification strategy based on ordered heteroskedasticity. This approach builds on the foundational framework of Rigobon

[1] Available at https://epaper.cs.com.cn/zgzqb/images/2008-06/10/A03/ZQBA0030610C.pdf

(2003) and the insight of Rigobon and Sack (2004) that "*the variance of monetary policy shocks is higher...when a larger portion of the news hitting markets is about monetary policy.*" This establishes the core principle that greater news intensity leads to higher shock variance. Our key intuition follows directly: for any given target shock, its variance is highest on announcements where it is the explicit, "loud" focus, compared to announcements where it is only implicitly signaled. Formally, the quantity-target (Q-target) shock exhibits higher variance on quantity-target-based announcement (Q-announcement) days than on price-target-based announcement (P-announcement) days, and vice versa for the price-target (P-target) shock. Without loss of generality, we also assume that the variance of the silent-news shock for a given target is no less than its level in the absence of policy announcements, as a flexible and natural condition. As summarized in Table 1, this "within-shock" variance ordering provides a robust basis not only for identifying the unobserved shocks precipitated by monetary policy news but also for systematically disentangling the two policy shocks and assigning them clear economic labels. Thereby, it directly solves the labeling problem that has challenged heteroskedasticity-based methods in multi-shock settings (Lewis, 2021).

Table 1: Loud and Silent News in China's Monetary Policy (MP) Announcements

Event Type	MP Announcement	Q-Target Shock μ_t^Q $\sigma_Q^2 \equiv \text{Var}(\mu_t^Q)$	P-Target Shock μ_t^P $\sigma_P^2 \equiv \text{Var}(\mu_t^P)$
0	None	$\sigma_{Q,0}^2$ (No news)	$\sigma_{P,0}^2$ (No news)
1	Q-announcement	$\sigma_{Q,l}^2$ (Loud news)	$\sigma_{P,s}^2$ (Silent news)
2	P-announcement	$\sigma_{Q,s}^2$ (Silent news)	$\sigma_{P,l}^2$ (Loud news)
Variance Ordering		$\sigma_{Q,l}^2 > \sigma_{Q,s}^2 \geq \sigma_{Q,0}^2$	$\sigma_{P,l}^2 > \sigma_{P,s}^2 \geq \sigma_{P,0}^2$

Note: This table defines the notation for the variance of structural shocks under the ordered-heteroskedasticity assumption. Event Type 0 represents non-announcement days; Event Type 1 represents quantity-target-based (Q-) announcement days; Event Type 2 represents price-target-based (P-) announcement days. μ_t^Q and μ_t^P denote the quantity-target and price-target shocks, respectively. Their variances are denoted as $\sigma_Q^2 \equiv \text{Var}(\mu_t^Q)$ and $\sigma_P^2 \equiv \text{Var}(\mu_t^P)$. The subscripts l, s, and 0 denote the variance regime: whether the shock corresponds to the loud-news (l), silent-news (s), or no-news (0) regime, respectively. The final row states the core variance ordering assumption.

Applying this method to Chinese Treasury bond yields, we find that the dual-shock specification significantly outperforms the traditional single-shock specification. Our key empirical results reveal that: (1) quantity-target shocks exert a stronger impact on short-term yields, whereas the effect of price-target shocks increases with bond maturity; (2) silent news, particularly implicit price signals within quantity announcements, provides powerful forward guidance and significantly predicts future policy adjustments; and (3) both explicit and implicit target shocks trigger significant and persistent responses in bond yields and money market rates.

Our study makes three primary contributions. Methodologically, we reframe the essence of heteroskedasticity from a simple change in variance to a systematic ordering of variances, which directly reflects the intensity of specific news flows. By formalizing this ordered-heteroskedasticity strategy, we extend the core insight of Rigobon (2003) and demonstrate the strategy's central role in solving the shock labeling problem. Empirically, we are the first to rigorously identify and label dual-target shocks from PBoC announcements, challenging the prevailing single-shock paradigm and offering new insights into China's monetary policy transmission mechanism. Practically, our findings elucidate the potency of silent news, with direct implications for the PBoC's communication strategy and for global investors seeking to decode China's policy signals.

Looking ahead, our framework also holds promise for analyzing future policy regimes. As the PBoC shifts its primary policy rate anchor toward the short end of the maturity spectrum (e.g., the 7-day reverse repo rate), the transmission patterns of quantity- and price-target shocks may converge. Specifically, both types of shocks could exhibit similarly monotonic, declining impact coefficients across bond maturities. This convergence in the term structure of their effects would make the two shocks statistically harder to distinguish, severely undermining the efficacy of traditional identification frameworks that rely on distinct impact patterns. In contrast, our ordered-heteroskedasticity strategy, which exploits differences in shock variance across announcement types rather than differences in yield curve responses, remains theoretically robust and applicable even under such evolving conditions.

The remainder of the paper proceeds as follows. Section 2 reviews the related literature. Section 3 details the model, identification strategy, and estimation method. Section 4 describes the data. Section 5 presents the empirical results, and Section 6 concludes.

2 Literature Review

Our research is situated at the intersection of two active strands of literature: the identification of multiple dimensions in monetary policy shocks, and the application of heteroskedasticity-based methods for high-frequency shock identification. This section reviews the key contributions and limitations of these literatures, highlighting the specific gaps our study aims to fill.

2.1 The Multidimensionality of Monetary Policy Announcement Shocks

Early research on monetary policy announcements largely adhered to a single-shock paradigm. Seminal studies, such as Cook and Hahn (1989), assessed market reactions by equating policy shocks with changes in the federal funds rate target. Kuttner (2001) advanced this approach by decomposing target changes into anticipated and unanticipated components using federal funds futures, firmly establishing that asset prices primarily respond to surprise elements. While foundational, these studies implicitly assumed that announcements conveyed only one type of information—the immediate setting of the policy rate.

A pivotal shift in understanding occurred with Gürkaynak et al. (2005), who demonstrated that a single factor is insufficient to capture the full impact of FOMC announcements on the yields. By analyzing the joint response of federal funds futures and Eurodollar futures, they extracted two distinct factors: a "target factor", representing the unexpected change in the current federal funds rate, and a "path factor", reflecting revisions to the expected future path of monetary policy. Their critical finding was that the path factor often exerts a more substantial influence on longer-term yields than the target factor itself, underscoring the importance of moving beyond a single-dimensional framework. This seminal work has inspired extensive subsequent research on identifying dual or even triple impacts of monetary announcements (e.g., Brand et al., 2010; Campbell et al., 2012; Gertler and Karadi, 2015; Altavilla et al., 2019; Kaminska et al., 2021; Andrade and Ferroni, 2021; Swanson, 2021; Swanson and Jayawickrema, 2024, among others).

However, this influential identification frameworks are not directly applicable to China's context. They typically rely on the existence of deep derivative markets, such as federal funds futures, to directly observe and measure market expectations for policy targets. China lacks equivalent financial instruments for its quantity-target-based tools (e.g., RRR futures) and only developed limited derivatives for its price tools.

An alternative identification strategy, which treats the target shock as unobservable and imposes theory-based constraints on its impact coefficients (Cieslak and Schrimpf, 2019; Jarociński and Karadi, 2020; Andrade and Ferroni, 2021), is designed for environments with only one operational target, either for the federal funds rate before Zero Lower Bound (ZLB) period or Large-Scale Asset Purchases (LSAP). China's dual-target framework, by contrast, is inherent and concurrent. Existing strategies fail to account for the synergistic coordination between these continuously employed tools, which generates dual-target shocks from a single announcement.

Moreover, a closer examination reveals a more fundamental disconnect: the predominant explanations for shock multidimensionality in the literature do not align with the Chinese context. These explanations typically arise from two distinct mechanisms.

The first mechanism attributes multidimensionality to supplementary information embedded in the announcements beyond the stated target. Empirical foundations for this view were laid by Gürkaynak et al. (2005), who found that the path factor was primarily realized on FOMC statement days, and by Nakamura and Steinsson (2018), who argued that the Fed's communication shaped broader economic expectations beyond immediate rate changes. Further evidence comes from Lunsford (2020), who showed that the linguistic nature of forward guidance systematically shapes private-sector responses. Gürkaynak et al. (2020) reconceptualized these insights formally, framing multiple shocks as originating from the announcement's own information structure—contrasting "headline" and "non-headline" news. However, as illustrated in Appendix A.1, PBoC announcements are characteristically terse, containing only the factual adjustment of a specific policy tool and lacking the elaborate forward-looking text that would generate distinct non-headline news. Thus, this channel of multidimensionality appears inactive in China's context.

The second mechanism is the sequential adoption of new policy tools. Li et al. (2024) demonstrates that U.S. monetary policy shocks evolved from being effectively one-dimensional before 2008 to two-dimensional after the Global Financial Crisis, following the introduction of quantitative easing (QE) as a distinct second tool. While differing on the number of factors, studies such as Altavilla et al. (2019) and Swanson (2021) similarly identify an additional shock dimension during the QE period. This genesis—adding a new tool to a pre-existing framework—contrasts sharply with China's setting, where multidimensionality arises not from tool addition but from the market's inference regarding the synergistic coordination between two inherently and continuously employed tools. Consequently, the dual shocks from a PBoC announcement reflect a distinct mechanism whereby adjusting one tool implicitly signals the stance of the other—a feature that existing frameworks are neither designed to identify nor equipped to explain.

2.2 Heteroskedasticity-Based Identification of Monetary Policy Announcement Shocks

The second relevant literature employs heteroskedasticity for identification, offering a solution to the challenge of robust identification assumption. The foundational insight, established by Rigobon (2003), is that the variance of monetary policy shocks increases on days with major policy announcements, a pattern that has been leveraged to identify the effects of monetary policy news (Rigobon and Sack, 2004; Wright, 2012; Bu et al., 2021). By comparing the variance-covariance matrices of asset returns during announcement windows to those from non-announcement periods, one can identify the impact of structural shocks without imposing potentially invalid parameter restrictions such as exclusion, sign, or long-run restrictions. And the identified shock can naturally be labeled as monetary policy shock. This makes it particularly valuable for contexts like China, where derivative markets for policy expectations are absent (Lin and Niu, 2021).

Extending this logic to multi-shock settings is conceptually straightforward. Gürkaynak et al. (2020), for instance, used heteroskedasticity to separate non-headline from headline news shocks, showing that the latter explained a larger share of variance in long-term yields. Lewis (2021) proposed a novel method for shock identification using stochastic volatility, which shared a similar spirit with heteroskedasticity-based approaches; this method was subsequently applied by Lewis (2025) to identify multiple monetary policy shocks from FOMC announcements.

However, heteroskedasticity-based identification strategies in multi-shock settings face a critical "labeling" limitation (Lewis, 2021). While heteroskedasticity can help identify statistically distinct shocks, it cannot intrinsically assign them clear economic interpretations (e.g., which shock corresponds to a quantity tool vs. a price tool).[2] Resolving this typically requires appealing to external information. For example, Gürkaynak et al. (2020) reviewed financial press commentary related to the five largest realizations of their identified non-headline news and classified them as "statement surprises". Lewis (2025) assigned shock labels by drawing on historical decomposition results and economic theory. These examples suggest that, to facilitate meaningful economic interpretation, heteroskedasticity-based identification may ultimately require grounding in economic reasoning, which is a non-trivial task for a non-standard framework like that of China.

2.3 Synthesizing the Gaps and Our Contribution

A synthesis of these two literatures reveals a critical gap, particularly for analyzing economic policies such as China's. While the first literature establishes the importance of multi-dimensional shocks and the second provides a methodology to identify them with-

[2]More broadly, identification strategies that rely solely on statistical properties of the data—even robust ones—also encounter a labeling challenge and require further analysis to assign economic meaning to the shocks. For instance, Lanne et al. (2010) modeled VAR residuals using Markov-switching and conditional heteroskedasticity, while Jarociński (2024) assumed t-distributed shocks, among others.

out derivatives, the two have not been successfully fused in a way that both identifies and economically labels multiple shocks in a dual-tool framework.

Our study bridges this gap. We adopt the core premise from the first literature—that tool multiplicity leads to shock multiplicity—and adapt it to China's inherent dual-tool setting. From the second literature, we leverage the heteroskedasticity-based identification strategy but augment it with our ordered-heteroskedasticity assumption. This innovation directly addresses the labeling problem by using the type of policy announcement (quantity- vs. price-target-based) to impose an intuitive variance ordering on the shocks, thereby assigning them clear economic labels as quantity-target or price-target shocks. This tailored strategy allows us to open the "black box" of China's monetary policy announcements and formally test for the presence and effects of dual shocks, a task beyond the reach of existing methodologies.

3 Heteroskedasticity Identification and Estimation

3.1 Model Setting

We assume that the yield vector $\boldsymbol{Y}_t$ of n Treasury bond yields with different maturities follows a p-th order vector autoregression (VAR), as shown in Equation (1):

$$\boldsymbol{Y}_t = \boldsymbol{c} + \sum_{i=1}^{p} \boldsymbol{\Phi}_i \boldsymbol{Y}_{t-i} + \boldsymbol{\varepsilon}_t. \tag{1}$$

The residuals in $\boldsymbol{\varepsilon}_t$ are determined by a vector of orthogonal structural shocks $\boldsymbol{\mu_t}$, which contains quantity-target shock μ_t^Q, price-target shock μ_t^P, and other structural shocks $\boldsymbol{\mu}_t^+$, which exhibit zero cross-variance, as indicated in Equations (2) and (3):

$$\boldsymbol{\varepsilon}_t = \boldsymbol{B}\boldsymbol{\mu_t} = \boldsymbol{B}\begin{pmatrix} \mu_t^Q \\ \mu_t^P \\ \boldsymbol{\mu}_t^+ \end{pmatrix}, \mathrm{Cov}(\boldsymbol{\mu}_t^+, \mu_t^Q) = \mathrm{Cov}(\boldsymbol{\mu}_t^+, \mu_t^P) = \mathbf{0}_{(n-2)\times 1}, \mathrm{Cov}(\mu_t^Q, \mu_t^P) = 0, \tag{2}$$

$$\boldsymbol{B} = \begin{pmatrix} \boldsymbol{\alpha}, & \boldsymbol{\beta}, & \boldsymbol{\Gamma} \end{pmatrix}, \quad \boldsymbol{\alpha} = \begin{pmatrix} \alpha_1 \\ \vdots \\ \alpha_n \end{pmatrix}, \quad \boldsymbol{\beta} = \begin{pmatrix} \beta_1 \\ \vdots \\ \beta_n \end{pmatrix}, \quad \boldsymbol{\Gamma} = \begin{pmatrix} \gamma_1^1 & \cdots & \gamma_1^{n-2} \\ \vdots & \ddots & \vdots \\ \gamma_n^1 & \cdots & \gamma_n^{n-2} \end{pmatrix}. \tag{3}$$

In the impact coefficient matrix $\boldsymbol{B}$ of structural shocks, $\boldsymbol{\alpha}$ and $\boldsymbol{\beta}$ are the impact coefficient vectors of the quantity-target shock and price-target shock, respectively, and $\boldsymbol{\Gamma}$ is the impact coefficient matrix of other structural shocks. To ensure the ability to identify structural shocks from the reduced-form residuals $\boldsymbol{\varepsilon}_t$, we assume that the matrix $\boldsymbol{B}$ has full rank.

3.2 Ordered Heteroskedasticity

This section formalizes the dual-shock heteroskedasticity specification, building upon the model setup in Equations (1) to (3) and the intuitive framework presented in Table 1. This structure allows us to identify and economically label the shocks based on their variance patterns across three different announcement events:

- Event 0: Non-monetary policy announcement days.
- Event 1: Quantity-target-based announcement (Q-announcement) days.
- Event 2: Price-target-based announcement (P-announcement) days.

Equations (4) to (6) present the heteroskedasticity specification of shocks, referred to as the dual-shock specification hereafter. Equation (4) establishes different variances based on the type of monetary policy announcement event. $\sigma^2_{Q,i}$ and $\sigma^2_{P,i}$ (for $i = 0, l, s$) represent the variances of quantity-target shock and price-target shock under different events, respectively. Consistent with traditional heteroskedasticity assumptions, we assume that the other structural shocks $\boldsymbol{\mu}_t^+$, which are unrelated to monetary policy shocks, do not exhibit variance changes between monetary policy announcement days (Event 1 and 2) and non-announcement days (Event 0), with variance standardized to 1.

$$\mathrm{Var}(\mu_t^Q) = \begin{cases} \sigma^2_{Q,0} & \text{Event } 0 \\ \sigma^2_{Q,l} & \text{Event } 1 \\ \sigma^2_{Q,s} & \text{Event } 2 \end{cases}, \quad \mathrm{Var}(\mu_t^P) = \begin{cases} \sigma^2_{P,0} & \text{Event } 0 \\ \sigma^2_{P,s} & \text{Event } 1 \\ \sigma^2_{P,l} & \text{Event } 2 \end{cases}, \quad \mathrm{Var}(\boldsymbol{\mu}_t^+) = \boldsymbol{I}_{(n-2)\times(n-2)}. \tag{4}$$

The core of our identification strategy lies in the ordered-heteroskedasticity assumptions for the policy shocks:

$$\sigma^2_{Q,l} > \sigma^2_{Q,s} \geq \sigma^2_{Q,0}, \tag{5}$$

$$\sigma^2_{P,l} > \sigma^2_{P,s} \geq \sigma^2_{P,0}. \tag{6}$$

3.2.1 Interpretation of Variance Ordering

The inequalities in Equation (5) and (6) provide the necessary restrictions for shock identification and labeling. For quantity-target shock μ_t^Q, Equation (5) embodies three key assumptions:

- $\sigma^2_{Q,l} > \sigma^2_{Q,0}$ (Loud-news heteroskedasticity): On Q-announcement days (Event 1), the variance of μ_t^Q is larger than on non-announcement days (Event 0). This arises because Q-announcements explicitly disclose quantity adjustments (e.g., RRR changes), providing concentrated information that amplifies shock volatility.

- $\sigma^2_{Q,s} \geq \sigma^2_{Q,0}$ (Silent-news heteroskedasticity): On P-announcement days (Event 2), silent news may raise variance of quantity-target shock (i.e., $\sigma^2_{Q,s} > \sigma^2_{Q,0}$), but equality is not ruled out (i.e., $\sigma^2_{Q,s} = \sigma^2_{Q,0}$). This flexibility accommodates scenarios where implicit signals are too weak to alter market volatility, avoiding over-constraining the model.

- $\sigma^2_{Q,l} > \sigma^2_{Q,s}$ (Ordered-heteroskedasticity between loud and silent news): On P-announcement days (Event 2), μ_t^Q acts as silent news—investors infer quantity-related signals indirectly from price adjustments (e.g., BLDR changes) rather than from explicit quantity targets. Thus, the variance of μ_t^Q is smaller than on Q-announcement days, reflecting the difference in information content between loud and silent news regarding the quantity target.

Here, the first two conditions are the typical heteroskedasticity assumptions that the variance on announcement days exceeds (or no less than) that on non-announcement days ($\sigma^2_{Q,l} > \sigma^2_{Q,0}$, $\sigma^2_{Q,s} \geq \sigma^2_{Q,0}$), reflecting the foundational insight of Rigobon (2003) that the variance of asset price innovations increases on days with major policy announcements. The third condition that the variance of a shock is higher when it is the loud news than when it is the silent news ($\sigma^2_{Q,l} > \sigma^2_{Q,s}$) is the core of our ordered-heteroskedasticity strategy, capturing the difference in information intensity between loud and silent news.

Likewise, Equation (6) applies the same logic to price-target shock μ_t^P.

These ordered-heteroskedasticity assumptions enable us to formally categorize loud and silent news, thereby resolving the classical labeling problem. The core rationale for employing heteroskedasticity in event studies is that an increase in variance captures the intensity of information arrival, which inherently defines a shock's label.[3] Our approach extends this principle by exploiting the ordering of shock variances to identify their origin during announcement events, grounded in the premise that loud news carries greater information intensity than silent news. Consequently, the label associated with the loud news is naturally assigned to the shock.

[3] The idea of using changes in asset price variance to proxy for information arrival can be traced back to Clark (1973), as summarized by Ghysels et al. (1996).

3.2.2 Conditional Moments Representation

To prepare for the identification analysis, we can first obtain the resulting variance-covariance matrices of the reduced-form residuals in Equation (1), based on the above dual-shock specifications, as follows:

$$\mathrm{Var}(\boldsymbol{\varepsilon}_t) = \begin{cases} \boldsymbol{\Sigma}_0 = \sigma^2_{Q,0}\boldsymbol{\alpha}\boldsymbol{\alpha}' + \sigma^2_{P,0}\boldsymbol{\beta}\boldsymbol{\beta}' + \boldsymbol{\Gamma}\boldsymbol{\Gamma}' & \text{Event 0} \\ \boldsymbol{\Sigma}_1 = \sigma^2_{Q,l}\boldsymbol{\alpha}\boldsymbol{\alpha}' + \sigma^2_{P,s}\boldsymbol{\beta}\boldsymbol{\beta}' + \boldsymbol{\Gamma}\boldsymbol{\Gamma}' & \text{Event 1} \\ \boldsymbol{\Sigma}_2 = \sigma^2_{Q,s}\boldsymbol{\alpha}\boldsymbol{\alpha}' + \sigma^2_{P,l}\boldsymbol{\beta}\boldsymbol{\beta}' + \boldsymbol{\Gamma}\boldsymbol{\Gamma}' & \text{Event 2} \end{cases}. \tag{7}$$

By comparing the variance-covariance matrices of Treasury bond yields across different event days, we obtain the following moment conditions:

$$\Delta\boldsymbol{\Sigma}_1 = \boldsymbol{\Sigma}_1 - \boldsymbol{\Sigma}_0 = \boldsymbol{\alpha}\boldsymbol{\alpha}'(\sigma^2_{Q,l} - \sigma^2_{Q,0}) + \boldsymbol{\beta}\boldsymbol{\beta}'(\sigma^2_{P,s} - \sigma^2_{P,0}), \tag{8}$$

$$\Delta\boldsymbol{\Sigma}_2 = \boldsymbol{\Sigma}_2 - \boldsymbol{\Sigma}_0 = \boldsymbol{\alpha}\boldsymbol{\alpha}'(\sigma^2_{Q,s} - \sigma^2_{Q,0}) + \boldsymbol{\beta}\boldsymbol{\beta}'(\sigma^2_{P,l} - \sigma^2_{P,0}), \tag{9}$$

where $\boldsymbol{\Delta\Sigma}_1$ denotes the difference in yield residual variance-covariance matrices between Q-announcement days and non-announcement days and $\boldsymbol{\Delta\Sigma}_2$ denotes the difference between P-announcement days and non-announcement days.

Since the four variance differentials, $\sigma^2_{Q,l} - \sigma^2_{Q,0}$, $\sigma^2_{P,s} - \sigma^2_{P,0}$, $\sigma^2_{Q,s} - \sigma^2_{Q,0}$ and $\sigma^2_{P,l} - \sigma^2_{P,0}$, in Equations (8) and (9) cannot be identified simultaneously, we standardize these moment conditions by imposing $\sigma^2_{Q,l} - \sigma^2_{Q,0} = 1$, as it is guaranteed to be positive by the ordering condition in Equation (5), and setting $\sigma^2_{Q,s} - \sigma^2_{Q,0} = \tilde{\sigma}^2_{Q,s}$ to be a free parameter that belongs to [0,1). Similarly, we set $\sigma^2_{P,l} - \sigma^2_{P,0} = 1$, and $\sigma^2_{P,s} - \sigma^2_{P,0} = \tilde{\sigma}^2_{P,s} \in [0, 1)$.

Using the above standardization conditions, we can obtain the following moment conditions required for shock identification:

$$\Delta\boldsymbol{\Sigma}_1 = \boldsymbol{\alpha}\boldsymbol{\alpha}' + \boldsymbol{\beta}\boldsymbol{\beta}'\tilde{\sigma}^2_{P,s}, \tag{10}$$

$$\Delta\boldsymbol{\Sigma}_2 = \boldsymbol{\alpha}\boldsymbol{\alpha}'\tilde{\sigma}^2_{Q,s} + \boldsymbol{\beta}\boldsymbol{\beta}'. \tag{11}$$

Thus, we are left with estimating the impact coefficients ($\boldsymbol{\alpha}$ and $\boldsymbol{\beta}$) and silent news jump parameters ($\tilde{\sigma}^2_{P,s}$ and $\tilde{\sigma}^2_{Q,s}$).

3.3 Identification Analysis

This section establishes the formal identifiability of our model parameters under the ordered-heteroskedasticity assumptions in the dual-shock specification. We propose that the parameters ($\boldsymbol{\alpha}$, $\boldsymbol{\beta}$, $\tilde{\sigma}^2_{Q,s}$, $\tilde{\sigma}^2_{P,s}$) are uniquely determined (up to sign changes in $\boldsymbol{\alpha}$ and $\boldsymbol{\beta}$) by the moment conditions and parameter restrictions derived from our framework.

Proposition 1. Given that $0 \leq \tilde{\sigma}^2_{P,s} < 1$ and $0 \leq \tilde{\sigma}^2_{Q,s} < 1$, then if the parameters $\boldsymbol{\alpha}$, $\boldsymbol{\beta}$, $\tilde{\sigma}^2_{Q,s}$, and $\tilde{\sigma}^2_{P,s}$ that satisfy the moment conditions in Equations (10) and (11) exist, they are unique (disregarding the overall sign change of vectors $\boldsymbol{\alpha}$ and $\boldsymbol{\beta}$).

Proof. Let $\boldsymbol{\alpha}$, $\boldsymbol{\beta}$, $\tilde{\sigma}^2_{Q,s}$, and $\tilde{\sigma}^2_{P,s}$ be a set of parameters satisfying Equations (10) and (11). To prove uniqueness, we consider three mutually exclusive cases based on the values of $\tilde{\sigma}^2_{Q,s}$ and $\tilde{\sigma}^2_{P,s}$.

(a) Both $\tilde{\sigma}^2_{Q,s}$ and $\tilde{\sigma}^2_{P,s}$ are zero.

In this case, the moment conditions simplify to:

$$\Delta\boldsymbol{\Sigma}_1 = \boldsymbol{\alpha}\boldsymbol{\alpha}', \tag{12}$$

$$\Delta\boldsymbol{\Sigma}_2 = \boldsymbol{\beta}\boldsymbol{\beta}'. \tag{13}$$

Suppose there exists an alternative set of parameters $\boldsymbol{\alpha}^*$, $\boldsymbol{\beta}^*$, $\tilde{\sigma}^{*2}_{Q,s}$, and $\tilde{\sigma}^{*2}_{P,s}$ that also satisfy Equations (10) and (11). It can be shown that if $\tilde{\sigma}^{*2}_{P,s} \neq 0$, it leads to a proportionality condition between $\boldsymbol{\alpha}^*$ and $\boldsymbol{\beta}^*$ that violates the full-rank assumption of the impact matrix $\boldsymbol{B}$. Therefore, we must have $\tilde{\sigma}^{*2}_{P,s} = 0$, and by symmetry, $\tilde{\sigma}^{*2}_{Q,s} = 0$. Consequently, $\boldsymbol{\alpha}\boldsymbol{\alpha}' = \boldsymbol{\alpha}^*\boldsymbol{\alpha}^{*\prime}$ and $\boldsymbol{\beta}\boldsymbol{\beta}' = \boldsymbol{\beta}^*\boldsymbol{\beta}^{*\prime}$, implying $\boldsymbol{\alpha} = \pm\boldsymbol{\alpha}^*$ and $\boldsymbol{\beta} = \pm\boldsymbol{\beta}^*$.

A detailed proof is as follows. Given $\boldsymbol{\alpha}^*$, $\boldsymbol{\beta}^*$, $\tilde{\sigma}^{*2}_{Q,s}$, and $\tilde{\sigma}^{*2}_{P,s}$ also satisfy Equations (10) and (11), we have:

$$\boldsymbol{\alpha}\boldsymbol{\alpha}' = \Delta\boldsymbol{\Sigma}_1 = \boldsymbol{\alpha}^*\boldsymbol{\alpha}^{*\prime} + \boldsymbol{\beta}^*\boldsymbol{\beta}^{*\prime}\tilde{\sigma}^{*2}_{Q,s}, \tag{14}$$

$$\boldsymbol{\beta}\boldsymbol{\beta}' = \Delta\boldsymbol{\Sigma}_2 = \boldsymbol{\alpha}^*\boldsymbol{\alpha}^{*\prime}\tilde{\sigma}^{*2}_{Q,s} + \boldsymbol{\beta}^*\boldsymbol{\beta}^{*\prime}. \tag{15}$$

Based on the properties of outer product $\boldsymbol{\alpha}\boldsymbol{\alpha}'$, we have

$$(\boldsymbol{\alpha}\boldsymbol{\alpha}')_{11} \times (\boldsymbol{\alpha}\boldsymbol{\alpha}')_{ii} = (\boldsymbol{\alpha}\boldsymbol{\alpha}')_{i1} \times (\boldsymbol{\alpha}\boldsymbol{\alpha}')_{1i}\,, \tag{16}$$

where $(\cdot)_{ij}$ denotes the (i, j) element of the matrix, and by symmetry, $(\boldsymbol{\alpha}\boldsymbol{\alpha}')_{ij} = (\boldsymbol{\alpha}\boldsymbol{\alpha}')_{ji}$.

Applying these properties to the right-hand side of Equation (14), we obtain

$$(\boldsymbol{\alpha}_1^*\boldsymbol{\alpha}_1^* + \boldsymbol{\beta}_1^*\boldsymbol{\beta}_1^*\tilde{\sigma}_{P,s}^{*2})(\boldsymbol{\alpha}_i^*\boldsymbol{\alpha}_i^* + \boldsymbol{\beta}_i^*\boldsymbol{\beta}_i^*\tilde{\sigma}_{P,s}^{*2}) = (\boldsymbol{\alpha}_1^*\boldsymbol{\alpha}_i^* + \boldsymbol{\beta}_1^*\boldsymbol{\beta}_i^*\tilde{\sigma}_{P,s}^{*2})^2. \tag{17}$$

Rearranging both sides leads to:

$$\boldsymbol{\alpha}_1^*\boldsymbol{\alpha}_1^*\boldsymbol{\beta}_i^*\boldsymbol{\beta}_i^*\tilde{\sigma}_{P,s}^{*2} + \boldsymbol{\alpha}_i^*\boldsymbol{\alpha}_i^*\boldsymbol{\beta}_1^*\boldsymbol{\beta}_1^*\tilde{\sigma}_{P,s}^{*2} = 2\boldsymbol{\alpha}_1^*\boldsymbol{\alpha}_i^*\boldsymbol{\beta}_1^*\boldsymbol{\beta}_i^*\tilde{\sigma}_{P,s}^{*2}. \tag{18}$$

If $\tilde{\sigma}_{P,s}^{*2} \neq 0$, then dividing Equation (18) by it gives:

$$\boldsymbol{\alpha}_1^*\boldsymbol{\alpha}_1^*\boldsymbol{\beta}_i^*\boldsymbol{\beta}_i^* + \boldsymbol{\alpha}_i^*\boldsymbol{\alpha}_i^*\boldsymbol{\beta}_1^*\boldsymbol{\beta}_1^* - 2\boldsymbol{\alpha}_1^*\boldsymbol{\alpha}_i^*\boldsymbol{\beta}_1^*\boldsymbol{\beta}_i^* = (\boldsymbol{\alpha}_1^*\boldsymbol{\beta}_i^* - \boldsymbol{\alpha}_i^*\boldsymbol{\beta}_1^*)^2 = 0. \tag{19}$$

Thus, we obtain the equality

$$\boldsymbol{\alpha}_1^*\boldsymbol{\beta}_i^* = \boldsymbol{\alpha}_i^*\boldsymbol{\beta}_1^*, \tag{20}$$

which is equivalent to

$$\frac{\boldsymbol{\alpha}_1^*}{\boldsymbol{\beta}_1^*} = \frac{\boldsymbol{\alpha}_i^*}{\boldsymbol{\beta}_i^*}. \tag{21}$$

This implies that $\boldsymbol{\alpha}^*$ and $\boldsymbol{\beta}^*$ are linearly dependent, contradicting the full-rank requirement of the impact coefficient matrix $\boldsymbol{B}$. Thus $\tilde{\sigma}_{P,s}^{*2} = 0$, and by symmetry, $\tilde{\sigma}_{Q,s}^{*2} = 0$. Substituting these two zero values back into Equations (14) and (15) yields:

$$\boldsymbol{\alpha}\boldsymbol{\alpha}' = \Delta\boldsymbol{\Sigma}_1 = \boldsymbol{\alpha}^*\boldsymbol{\alpha}^{*\prime}, \tag{22}$$

$$\boldsymbol{\beta}\boldsymbol{\beta}' = \Delta\boldsymbol{\Sigma}_2 = \boldsymbol{\beta}^*\boldsymbol{\beta}^{*\prime}. \tag{23}$$

For outer products, this implies $\boldsymbol{\alpha} = \pm\boldsymbol{\alpha}^*$ and $\boldsymbol{\beta} = \pm\boldsymbol{\beta}^*$, confirming uniqueness up to sign.

(b) Exactly one of $\tilde{\sigma}_{Q,s}^2$ and $\tilde{\sigma}_{P,s}^2$ is zero.

Without loss of generality, we assume $\tilde{\sigma}_{P,s}^2 = 0$. If there exists an alternative set of parameters $\boldsymbol{\alpha}^*$, $\boldsymbol{\beta}^*$, $\tilde{\sigma}_{Q,s}^{*2}$, and $\tilde{\sigma}_{P,s}^{*2}$ that also satisfy Equations (10) and (11), then we have:

$$\boldsymbol{\alpha}\boldsymbol{\alpha}' = \Delta\boldsymbol{\Sigma}_1 = \boldsymbol{\alpha}^*\boldsymbol{\alpha}^{*\prime} + \boldsymbol{\beta}^*\boldsymbol{\beta}^{*\prime}\tilde{\sigma}_{P,s}^{*2}, \tag{24}$$

$$\boldsymbol{\alpha}\boldsymbol{\alpha}'\tilde{\sigma}_{Q,s}^2 + \boldsymbol{\beta}\boldsymbol{\beta}' = \Delta\boldsymbol{\Sigma}_2 = \boldsymbol{\alpha}^*\boldsymbol{\alpha}^{*\prime}\tilde{\sigma}_{Q,s}^{*2} + \boldsymbol{\beta}^*\boldsymbol{\beta}^{*\prime}. \tag{25}$$

Equation (24) has the same form as Equation (14). The same logic as Case (a) implies

$\tilde{\sigma}^{*2}_{P,s} = 0$ and $\boldsymbol{\alpha} = \pm\boldsymbol{\alpha}^*$. Substituting $\boldsymbol{\alpha} = \pm\boldsymbol{\alpha}^*$ into Equation (25) yields:

$$\boldsymbol{\beta}\boldsymbol{\beta}' = \boldsymbol{\alpha}^*\boldsymbol{\alpha}^{*\prime}(\tilde{\sigma}^{*2}_{Q,s} - \tilde{\sigma}^{2}_{Q,s}) + \boldsymbol{\beta}^*\boldsymbol{\beta}^{*\prime}. \tag{26}$$

Equation (26) also has similar form as Equation (15). Similarly, we can prove $\tilde{\sigma}^{*2}_{Q,s} - \tilde{\sigma}^{2}_{Q,s} = 0$ (i.e. $\tilde{\sigma}^{*2}_{Q,s} = \tilde{\sigma}^{2}_{Q,s}$) and $\boldsymbol{\beta} = \pm\boldsymbol{\beta}^*$. Thus, if $\tilde{\sigma}^{2}_{P,s} = 0$, we prove the uniqueness of $\tilde{\sigma}^{2}_{P,s}$ and $\tilde{\sigma}^{2}_{Q,s}$, and the uniqueness of $\boldsymbol{\alpha}$ and $\boldsymbol{\beta}$ up to sign change. By symmetry, we can prove that, if $\tilde{\sigma}^{2}_{Q,s} = 0$, $\tilde{\sigma}^{2}_{P,s}$ and $\tilde{\sigma}^{2}_{P,s}$ are also unique, and $\boldsymbol{\alpha}$ and $\boldsymbol{\beta}$ are unique up to sign change.

(c) Both $\tilde{\sigma}^{2}_{Q,s}$ and $\tilde{\sigma}^{2}_{P,s}$ are non-zero.

In this general case, we can redefine $\bar{\boldsymbol{\beta}} = \boldsymbol{\beta}\sqrt{\tilde{\sigma}^{2}_{P,s}}$ and $\omega^2_{P,s} = \frac{1}{\tilde{\sigma}^{2}_{P,s}}$ (noting that $\omega^2_{P,s} > 1$ since $0 < \tilde{\sigma}^{2}_{P,s} < 1$). Then Equations (10) and (11) can be rewritten as:

$$\Delta\boldsymbol{\Sigma}_1 = \boldsymbol{\alpha}\boldsymbol{\alpha}' + \bar{\boldsymbol{\beta}}\bar{\boldsymbol{\beta}}', \tag{27}$$

$$\Delta\boldsymbol{\Sigma}_2 = \boldsymbol{\alpha}\boldsymbol{\alpha}'\tilde{\sigma}^{2}_{Q,s} + \bar{\boldsymbol{\beta}}\bar{\boldsymbol{\beta}}'\omega^2_{P,s}. \tag{28}$$

The uniqueness of $\boldsymbol{\alpha}$, $\bar{\boldsymbol{\beta}}$, $\tilde{\sigma}^{2}_{Q,s}$ and $\omega^2_{P,s}$ in Equations (27) and (28) guarantees the uniqueness of $\boldsymbol{\alpha}$, $\boldsymbol{\beta}$, $\tilde{\sigma}^{2}_{Q,s}$ and $\tilde{\sigma}^{2}_{P,s}$ in Equations (10) and (11). This transformation enables us to recasts the system into a multi-regime heteroskedastic model that facilitates the proof of identification. We construct an invertible matrix:

$$\bar{\boldsymbol{B}} = (\boldsymbol{\alpha}, \bar{\boldsymbol{\beta}}, \bar{\boldsymbol{\Gamma}}), \tag{29}$$

and diagonal matrices $\boldsymbol{\Lambda}_1$ and $\boldsymbol{\Lambda}_2$ that contain the variance parameters:

$$\boldsymbol{\Lambda}_1 = \begin{pmatrix} 2 & 0 & 0 \\ 0 & 2 & 0 \\ 0 & 0 & \boldsymbol{I}_{(n-2)\times(n-2)} \end{pmatrix}, \quad \boldsymbol{\Lambda}_2 = \begin{pmatrix} \bar{\sigma}^2_{Q,s} & 0 & 0 \\ 0 & \bar{\omega}^2_{P,s} & 0 \\ 0 & 0 & \boldsymbol{I}_{(n-2)\times(n-2)} \end{pmatrix}, \tag{30}$$

where $\bar{\boldsymbol{\Gamma}}$ is any $n\times(n-2)$ matrix that ensures $\bar{\boldsymbol{B}}$ is invertible, $\boldsymbol{I}_{n-2}$ is the $(n-2)\times(n-2)$ identity matrix, $\bar{\sigma}^2_{Q,s} = \tilde{\sigma}^2_{Q,s} + 1 < 2$, and $\bar{\omega}^2_{P,s} = \omega^2_{P,s} + 1 > 2$. It is clear that these constructed matrices satisfy the following equations:

$$\bar{\boldsymbol{B}}\bar{\boldsymbol{B}}' = \Delta\boldsymbol{\Sigma}_1 + \bar{\boldsymbol{\Gamma}}\bar{\boldsymbol{\Gamma}}', \tag{31}$$

$$\bar{\boldsymbol{B}}\boldsymbol{\Lambda}_1\bar{\boldsymbol{B}}' = 2\Delta\boldsymbol{\Sigma}_1 + \bar{\boldsymbol{\Gamma}}\bar{\boldsymbol{\Gamma}}', \tag{32}$$

$$\bar{\boldsymbol{B}}\boldsymbol{\Lambda}_2\bar{\boldsymbol{B}}' = \Delta\boldsymbol{\Sigma}_2 + \Delta\boldsymbol{\Sigma}_1 + \bar{\boldsymbol{\Gamma}}\bar{\boldsymbol{\Gamma}}'. \tag{33}$$

Based on the construction of $\bar{\boldsymbol{B}}$, the right-hand sides of Equations (31)-(33) are all positive definite matrices.

Assuming an alternative set of parameters $\boldsymbol{\alpha}^*$, $\bar{\boldsymbol{\beta}}^*$, $\tilde{\sigma}^{*2}_{Q,s}$ and $\omega^{*2}_{P,s}$ exists, then using the same construction method, $\bar{\boldsymbol{B}}^* = (\boldsymbol{\alpha}^*, \bar{\boldsymbol{\beta}}^*, \bar{\boldsymbol{\Gamma}})$ and $\boldsymbol{\Lambda}_2^* = \begin{pmatrix} \bar{\sigma}^{*2}_{Q,s} & 0 & 0 \\ 0 & \bar{\omega}^{*2}_{P,s} & 0 \\ 0 & 0 & \boldsymbol{I}_{n-2} \end{pmatrix}$ are defined accordingly with $\bar{\sigma}^{*2}_{Q,s} = \tilde{\sigma}^{*2}_{Q,s} + 1 < 2$ and $\bar{\omega}^{*2}_{P,s} = \omega^{*2}_{P,s} + 1 > 2$. Similarly, these newly defined $\bar{\boldsymbol{B}}^*$ and $\boldsymbol{\Lambda}_2^*$ also satisfy the relationship characterized by Equations (31)-(33), such that these equations hold true if $\bar{\boldsymbol{B}}^*$ and $\boldsymbol{\Lambda}_2^*$ replace $\bar{\boldsymbol{B}}$ and $\boldsymbol{\Lambda}_2$ on the left-hand sides. Thus, we have:

$$\bar{\boldsymbol{B}}^*\bar{\boldsymbol{B}}^{*\prime} = \bar{\boldsymbol{B}}\bar{\boldsymbol{B}}', \tag{34}$$

$$\bar{\boldsymbol{B}}^*\boldsymbol{\Lambda}_1\bar{\boldsymbol{B}}^{*\prime} = \bar{\boldsymbol{B}}\boldsymbol{\Lambda}_1\bar{\boldsymbol{B}}', \tag{35}$$

$$\bar{\boldsymbol{B}}^*\boldsymbol{\Lambda}_2^*\bar{\boldsymbol{B}}^{*\prime} = \bar{\boldsymbol{B}}\boldsymbol{\Lambda}_2\bar{\boldsymbol{B}}'. \tag{36}$$

Next, we complete the proof to this case following Lanne et al. (2010)'s identification procedure. Equation (34) implies that $\bar{\boldsymbol{B}}^*$ is also invertible given $\bar{\boldsymbol{B}}$ as invertible. Then there exists a matrix $\boldsymbol{Q}$ such that $\bar{\boldsymbol{B}}^* = \bar{\boldsymbol{B}}\boldsymbol{Q}$. Substituting it into Equations (34) to (36) gives:

$$\bar{\boldsymbol{B}}\boldsymbol{Q}\boldsymbol{Q}'\bar{\boldsymbol{B}}' = \bar{\boldsymbol{B}}\bar{\boldsymbol{B}}', \tag{37}$$

$$\bar{\boldsymbol{B}}\boldsymbol{Q}\boldsymbol{\Lambda}_1\boldsymbol{Q}'\bar{\boldsymbol{B}}' = \bar{\boldsymbol{B}}\boldsymbol{\Lambda}_1\bar{\boldsymbol{B}}', \tag{38}$$

$$\bar{\boldsymbol{B}}\boldsymbol{Q}\boldsymbol{\Lambda}_2^*\boldsymbol{Q}'\bar{\boldsymbol{B}}' = \bar{\boldsymbol{B}}\boldsymbol{\Lambda}_2\bar{\boldsymbol{B}}'. \tag{39}$$

Equation (37) implies $\boldsymbol{Q}\boldsymbol{Q}' = \boldsymbol{I}$, such that $\boldsymbol{Q}$ is an orthogonal matrix. Equations (38) and (39) imply that $\boldsymbol{Q}\boldsymbol{\Lambda}_1\boldsymbol{Q}' = \boldsymbol{\Lambda}_1$ and $\boldsymbol{Q}\boldsymbol{\Lambda}_2^*\boldsymbol{Q}' = \boldsymbol{\Lambda}_2$, and post multiplying $\boldsymbol{Q}$ to both sides yields:

$$\boldsymbol{Q}\boldsymbol{\Lambda}_1 = \boldsymbol{\Lambda}_1\boldsymbol{Q}, \tag{40}$$

$$\boldsymbol{Q}\boldsymbol{\Lambda}_2^* = \boldsymbol{\Lambda}_2\boldsymbol{Q}. \tag{41}$$

By partitioning $\boldsymbol{Q}$ in Equation (40) and (41), we have:

$$\begin{pmatrix} Q_{11} & Q_{12} & \boldsymbol{Q}_{13} \\ Q_{21} & Q_{22} & \boldsymbol{Q}_{23} \\ \boldsymbol{Q}_{31} & \boldsymbol{Q}_{32} & \boldsymbol{Q}_{33} \end{pmatrix} \begin{pmatrix} 2 & 0 & \boldsymbol{0} \\ 0 & 2 & \boldsymbol{0} \\ \boldsymbol{0} & \boldsymbol{0} & \boldsymbol{I} \end{pmatrix} = \begin{pmatrix} 2 & 0 & \boldsymbol{0} \\ 0 & 2 & \boldsymbol{0} \\ \boldsymbol{0} & \boldsymbol{0} & \boldsymbol{I} \end{pmatrix} \begin{pmatrix} Q_{11} & Q_{12} & \boldsymbol{Q}_{13} \\ Q_{21} & Q_{22} & \boldsymbol{Q}_{23} \\ \boldsymbol{Q}_{31} & \boldsymbol{Q}_{32} & \boldsymbol{Q}_{33} \end{pmatrix}, \tag{42}$$

$$\begin{pmatrix} Q_{11} & Q_{12} & \boldsymbol{Q}_{13} \\ Q_{21} & Q_{22} & \boldsymbol{Q}_{23} \\ \boldsymbol{Q}_{31} & \boldsymbol{Q}_{32} & \boldsymbol{Q}_{33} \end{pmatrix} \begin{pmatrix} \bar{\sigma}^{*2}_{Q,s} & 0 & \mathbf{0} \\ 0 & \bar{\omega}^{*2}_{P,s} & \mathbf{0} \\ \mathbf{0} & \mathbf{0} & \boldsymbol{I} \end{pmatrix} = \begin{pmatrix} \bar{\sigma}^{2}_{Q,s} & 0 & \mathbf{0} \\ 0 & \bar{\omega}^{2}_{P,s} & \mathbf{0} \\ \mathbf{0} & \mathbf{0} & \boldsymbol{I} \end{pmatrix} \begin{pmatrix} Q_{11} & Q_{12} & \boldsymbol{Q}_{13} \\ Q_{21} & Q_{22} & \boldsymbol{Q}_{23} \\ \boldsymbol{Q}_{31} & \boldsymbol{Q}_{32} & \boldsymbol{Q}_{33} \end{pmatrix}. \tag{43}$$

By simplifying Equations (42) and (43), we find:

$$\begin{pmatrix} 2Q_{11} & 2Q_{12} & \boldsymbol{Q}_{13} \\ 2Q_{21} & 2Q_{22} & \boldsymbol{Q}_{23} \\ 2\boldsymbol{Q}_{31} & 2\boldsymbol{Q}_{32} & \boldsymbol{Q}_{33} \end{pmatrix} = \begin{pmatrix} 2Q_{11} & 2Q_{12} & 2\boldsymbol{Q}_{13} \\ 2Q_{21} & 2Q_{22} & 2\boldsymbol{Q}_{23} \\ \boldsymbol{Q}_{31} & \boldsymbol{Q}_{32} & \boldsymbol{Q}_{33} \end{pmatrix}, \tag{44}$$

$$\begin{pmatrix} \bar{\sigma}^{*2}_{Q,s}Q_{11} & \bar{\omega}^{*2}_{P,s}Q_{12} & \boldsymbol{Q}_{13} \\ \bar{\sigma}^{*2}_{Q,s}Q_{21} & \bar{\omega}^{*2}_{P,s}Q_{22} & \boldsymbol{Q}_{23} \\ \bar{\sigma}^{*2}_{Q,s}\boldsymbol{Q}_{31} & \bar{\omega}^{*2}_{P,s}\boldsymbol{Q}_{32} & \boldsymbol{Q}_{33} \end{pmatrix} = \begin{pmatrix} \bar{\sigma}^{2}_{Q,s}Q_{11} & \bar{\sigma}^{2}_{Q,s}Q_{12} & \bar{\sigma}^{2}_{Q,s}\boldsymbol{Q}_{13} \\ \bar{\omega}^{2}_{P,s}Q_{21} & \bar{\omega}^{2}_{P,s}Q_{22} & \bar{\omega}^{2}_{P,s}\boldsymbol{Q}_{23} \\ \boldsymbol{Q}_{31} & \boldsymbol{Q}_{32} & \boldsymbol{Q}_{33} \end{pmatrix}. \tag{45}$$

Examining Equation (44), we find $\boldsymbol{Q}_{13} = \boldsymbol{Q}_{31} = \boldsymbol{Q}_{23} = \boldsymbol{Q}_{32} = \mathbf{0}$.

Comparing the off-diagonal elements in the first two rows of Equation (45) implies:

$$\begin{cases} \bar{\sigma}^{*2}_{Q,s}Q_{21} = \bar{\omega}^{2}_{P,s}Q_{21} \\ \bar{\omega}^{*2}_{P,s}Q_{12} = \bar{\sigma}^{2}_{Q,s}Q_{12} \end{cases}. \tag{46}$$

Since $\bar{\sigma}^{*2}_{Q,s} < 2 < \bar{\omega}^{2}_{P,s}$ and $\bar{\sigma}^{2}_{Q,s} < 2 < \bar{\omega}^{*2}_{P,s}$, it follows that $Q_{21} = Q_{12} = 0$. Thus, all off-diagonal blocks of $\boldsymbol{Q}$ must be zero.

Comparing the diagonal elements in the first two rows of Equation (45) implies:

$$\begin{cases} \bar{\sigma}^{*2}_{Q,s}Q_{11} = \bar{\sigma}^{2}_{Q,s}Q_{11} \\ \bar{\omega}^{*2}_{P,s}Q_{22} = \bar{\omega}^{2}_{P,s}Q_{22} \end{cases}. \tag{47}$$

If $\bar{\sigma}^{*2}_{Q,s} \neq \bar{\sigma}^{2}_{Q,s}$, then $Q_{11} = 0$, which implies that all elements in the first column of $\boldsymbol{Q}$ are zero, contradicting the fact that $\boldsymbol{Q}$ is an orthogonal matrix. Therefore, $\bar{\sigma}^{*2}_{Q,s} = \bar{\sigma}^{2}_{Q,s}$ and $Q_{11} = \pm 1$ must hold. Similarly, $\bar{\omega}^{*2}_{P,s} = \bar{\omega}^{2}_{P,s}$ and $Q_{22} = \pm 1$ also hold.

Thus, the orthogonal matrix $\boldsymbol{Q}$ and $\boldsymbol{\Lambda}^*_2$ satisfying Equations (37) to (39) take the following forms:

$$\boldsymbol{Q} = \begin{pmatrix} \pm 1 & 0 & \mathbf{0} \\ 0 & \pm 1 & \mathbf{0} \\ \mathbf{0} & \mathbf{0} & \boldsymbol{Q}_{33} \end{pmatrix}, \quad \boldsymbol{\Lambda}^*_2 = \boldsymbol{\Lambda}_2, \tag{48}$$

where $\boldsymbol{Q}_{33}$ is an orthogonal matrix.

It is evident that, disregarding sign changes in $\boldsymbol{\alpha}$ and $\bar{\boldsymbol{\beta}}$, the parameters $\boldsymbol{\alpha}$, $\bar{\boldsymbol{\beta}}$, $\tilde{\sigma}^2_{Q,s}$ and $\omega^2_{P,s}$ are unique. This guarantees the uniqueness of $\boldsymbol{\alpha}$, $\boldsymbol{\beta}$, $\tilde{\sigma}^2_{Q,s}$ and $\tilde{\sigma}^2_{P,s}$ in Equations (10) and (11).

Having synthesized the proofs for all three cases, we conclude that the parameters $\boldsymbol{\alpha}$, $\boldsymbol{\beta}$, $\tilde{\sigma}^2_{Q,s}$ and $\tilde{\sigma}^2_{P,s}$ are uniquely identifiable up to sign change in $\boldsymbol{\alpha}$ and $\boldsymbol{\beta}$, completing the proof. □

Proposition 1 establishes that the moment conditions defined by Equations (10) and (11), together with the restrictions imposed on $\tilde{\sigma}^2_{Q,s}$ and $\tilde{\sigma}^2_{P,s}$, provide sufficient conditions to identify the shocks. It is worth noting that the restrictions $\tilde{\sigma}^2_{Q,s} < 1$ and $\tilde{\sigma}^2_{P,s} < 1$ serve a dual purpose: they not only provide the economic rationale for labeling the shocks, but are also mathematically crucial in the proof of *Proposition* 1.

The intrinsic link between these two roles lies in resolving the identification ambiguity. The variance ordering, formalized by $\tilde{\sigma}^2_{Q,s} < 1$ and $\tilde{\sigma}^2_{P,s} < 1$, assigns the label "loud" news (i.e. Q-target shock in Q-announcement and P-target shock in P-announcement) to the shock with larger variance.[4] This same economic criterion simultaneously breaks the permutation invariance in the mathematical structure of the model. Specifically, in the proof, these restrictions are used to show that $Q_{21} = 0$ and $Q_{12} = 0$ in the transformation matrix.[5] The zero off-diagonal elements eliminate the possibility of swapping the identities of the loud- and silent-news shocks through an orthogonal rotation, thereby ruling out permutation invariance and ensuring the shocks are uniquely identified.

3.4 Shock Series

Given the invertibility of the impact matrix $\boldsymbol{B}$ and the identifiability of the structural parameters, we can analytically recover the time series of structural shocks following the approach of Stock and Watson (2018). *Proposition* 2 delineates the procedure for computing the shock series under different announcement regimes.

Proposition 2. Under the model specification in Equations (2) to (4), let $\boldsymbol{\Sigma}_i$ (for $i = 0, 1, 2$) denote the variance-covariance matrix of the reduced-form residuals $\boldsymbol{\varepsilon}_t$ under different events. The structural shocks μ^Q_t and μ^P_t can be expressed as linear combinations of $\boldsymbol{\varepsilon}_t$:

[4]We distinguish between loud and silent news by imposing $\sigma^2_{Q,l} > \sigma^2_{Q,s}$ and $\sigma^2_{P,l} > \sigma^2_{P,s}$. After standardizing $\sigma^2_{Q,l} - \sigma^2_{Q,0} = 1$ and $\sigma^2_{P,l} - \sigma^2_{P,0} = 1$, these variance orderings translate into the restrictions $\tilde{\sigma}^2_{Q,s} = \sigma^2_{Q,s} - \sigma^2_{Q,0} < 1$ and $\tilde{\sigma}^2_{P,s} = \sigma^2_{P,s} - \sigma^2_{P,0} < 1$.

[5]The proof establishes that $Q_{21} = 0$ and $Q_{12} = 0$ by leveraging the inequalities $\bar{\sigma}^{*2}_{Q,s} < 2 < \bar{\omega}^2_{P,s}$ and $\bar{\sigma}^2_{Q,s} < 2 < \bar{\omega}^{*2}_{P,s}$, which themselves follow from the restrictions $\tilde{\sigma}^2_{Q,s} < 1$ and $\tilde{\sigma}^2_{P,s} < 1$.

$$\begin{pmatrix} \mu_t^Q \\ \mu_t^P \end{pmatrix} = \begin{pmatrix} \boldsymbol{A}_Q' \\ \boldsymbol{A}_P' \end{pmatrix} \boldsymbol{\varepsilon}_t, \tag{49}$$

where the loading vectors are conditional on the state of events,

$$\boldsymbol{A}_Q' = \begin{cases} \boldsymbol{\alpha}'\sigma_{Q,0}^2\boldsymbol{\Sigma}_0^{-1} & \text{Event } 0 \\ \boldsymbol{\alpha}'\sigma_{Q,l}^2\boldsymbol{\Sigma}_1^{-1} & \text{Event } 1 \\ \boldsymbol{\alpha}'\sigma_{Q,s}^2\boldsymbol{\Sigma}_2^{-1} & \text{Event } 2 \end{cases}, \quad \boldsymbol{A}_P' = \begin{cases} \boldsymbol{\beta}'\sigma_{P,0}^2\boldsymbol{\Sigma}_0^{-1} & \text{Event } 0 \\ \boldsymbol{\beta}'\sigma_{P,s}^2\boldsymbol{\Sigma}_1^{-1} & \text{Event } 1 \\ \boldsymbol{\beta}'\sigma_{P,l}^2\boldsymbol{\Sigma}_2^{-1} & \text{Event } 2 \end{cases}. \tag{50}$$

And the shock variances are given by:

$$\sigma_{Q,l}^2 = \frac{1}{\boldsymbol{\alpha}'\boldsymbol{\Sigma}_1^{-1}\boldsymbol{\alpha}}, \quad \sigma_{Q,s}^2 = \frac{1}{\boldsymbol{\alpha}'\boldsymbol{\Sigma}_2^{-1}\boldsymbol{\alpha}}, \quad \sigma_{P,l}^2 = \frac{1}{\boldsymbol{\beta}'\boldsymbol{\Sigma}_2^{-1}\boldsymbol{\beta}}, \quad \sigma_{P,s}^2 = \frac{1}{\boldsymbol{\beta}'\boldsymbol{\Sigma}_1^{-1}\boldsymbol{\beta}}. \tag{51}$$

Proof. Since $\boldsymbol{B}$ is invertible matrix by assumption, we have:

$$\begin{pmatrix} \mu_t^Q \\ \mu_t^P \\ \boldsymbol{\mu}_t^+ \end{pmatrix} = \boldsymbol{B}^{-1}\boldsymbol{\varepsilon}_t. \tag{52}$$

Equation (52) establishes that the structural shocks can be expressed as linear combinations of the reduced-form residuals, as demonstrated in Equation (49). By definition of $\boldsymbol{A}_Q$ as the loading vector of the quantity-target shock, we have:

$$\mathrm{Cov}(\mu_t^Q, \boldsymbol{\varepsilon}_t) = \mathrm{Cov}(\boldsymbol{A}_Q'\boldsymbol{\varepsilon}_t, \boldsymbol{\varepsilon}_t) = \boldsymbol{A}_Q'\mathrm{Var}(\boldsymbol{\varepsilon}_t), \tag{53}$$

$$\mathrm{Cov}(\mu_t^Q, \boldsymbol{\varepsilon}_t) = \mathrm{Cov}(\mu_t^Q, \boldsymbol{\alpha}\mu_t^Q + \boldsymbol{\beta}\mu_t^P + \boldsymbol{\Gamma}\boldsymbol{\mu}_t^+) = \boldsymbol{\alpha}'\mathrm{Var}(\mu_t^Q). \tag{54}$$

Equating these above expressions yields:

$$\boldsymbol{A}_Q'\mathrm{Var}(\boldsymbol{\varepsilon}_t) = \boldsymbol{\alpha}'\mathrm{Var}(\mu_t^Q). \tag{55}$$

Therefore, the loading vector of the quantity-target shock is:

$$\boldsymbol{A}_Q' = \boldsymbol{\alpha}'\mathrm{Var}(\mu_t^Q)\mathrm{Var}(\boldsymbol{\varepsilon}_t)^{-1} = \begin{cases} \boldsymbol{\alpha}'\sigma_{Q,0}^2\boldsymbol{\Sigma}_0^{-1} & \text{Event } 0 \\ \boldsymbol{\alpha}'\sigma_{Q,l}^2\boldsymbol{\Sigma}_1^{-1} & \text{Event } 1 \\ \boldsymbol{\alpha}'\sigma_{Q,s}^2\boldsymbol{\Sigma}_2^{-1} & \text{Event } 2 \end{cases}. \tag{56}$$

Similarly, for the loading vector of price-target shock $\boldsymbol{A}_P$:

$$\boldsymbol{A}_P' = \boldsymbol{\beta}'\mathrm{Var}(\mu_t^P)\mathrm{Var}(\boldsymbol{\varepsilon}_t)^{-1} = \begin{cases} \boldsymbol{\beta}'\sigma_{P,0}^2\boldsymbol{\Sigma}_0^{-1} & \text{Event 0} \\ \boldsymbol{\beta}'\sigma_{P,s}^2\boldsymbol{\Sigma}_1^{-1} & \text{Event 1} \\ \boldsymbol{\beta}'\sigma_{P,l}^2\boldsymbol{\Sigma}_2^{-1} & \text{Event 2} \end{cases}. \tag{57}$$

To derive the shock variances, consider:

$$\begin{aligned} \mathrm{Var}(\mu_t^Q) &= \boldsymbol{A}_Q'\mathrm{Var}(\boldsymbol{\varepsilon}_t)\boldsymbol{A}_Q, & (58) \\ &= \boldsymbol{\alpha}'\mathrm{Var}(\mu_t^Q)\mathrm{Var}(\boldsymbol{\varepsilon}_t)^{-1}\mathrm{Var}(\boldsymbol{\varepsilon}_t)\mathrm{Var}(\boldsymbol{\varepsilon}_t)^{-1}\mathrm{Var}(\mu_t^Q)\boldsymbol{\alpha}, & (59) \\ &= \boldsymbol{\alpha}'\mathrm{Var}(\boldsymbol{\varepsilon}_t)^{-1}\boldsymbol{\alpha}\mathrm{Var}(\mu_t^Q)^2. & (60) \end{aligned}$$

Solving for $\mathrm{Var}(\mu_t^Q)$ gives:

$$\mathrm{Var}(\mu_t^Q) = \frac{1}{\boldsymbol{\alpha}'\mathrm{Var}(\boldsymbol{\varepsilon}_t)^{-1}\boldsymbol{\alpha}}. \tag{61}$$

Thus, the event dependent variances of the quantity-target shock are:

$$\sigma_{Q,l}^2 = \frac{1}{\boldsymbol{\alpha}'\boldsymbol{\Sigma}_1^{-1}\boldsymbol{\alpha}}, \quad \sigma_{Q,s}^2 = \frac{1}{\boldsymbol{\alpha}'\boldsymbol{\Sigma}_2^{-1}\boldsymbol{\alpha}}. \tag{62}$$

Similarly, variances of the price-target shock are:

$$\sigma_{P,l}^2 = \frac{1}{\boldsymbol{\beta}'\boldsymbol{\Sigma}_2^{-1}\boldsymbol{\beta}}, \quad \sigma_{P,s}^2 = \frac{1}{\boldsymbol{\beta}'\boldsymbol{\Sigma}_1^{-1}\boldsymbol{\beta}}. \tag{63}$$

This completes the proof. □

3.5 Estimation Method

To implement our identification strategy empirically, we first model the dynamics of the yield vector $\boldsymbol{Y}_t$ using a VAR model. The optimal lag order for the VAR process is determined using the Bayesian and Akaike information criteria (BIC and AIC). In instances where these criteria suggest different orders, a likelihood ratio (LR) test is employed to select the final lag order, which in our application leads to a VAR(5) model.

Based on the VAR(5) residuals, the structural parameters—the impact coefficient vectors $(\boldsymbol{\alpha}, \boldsymbol{\beta})$ and the variance scaling factors for silent news $(\tilde{\sigma}_{Q,s}^2, \tilde{\sigma}_{P,s}^2)$—are estimated using the Generalized Method of Moments (GMM). The estimator solves the following minimum distance problem:

$$\hat{\boldsymbol{\Theta}} = \arg\min_{\boldsymbol{\Theta}=(\boldsymbol{\alpha},\boldsymbol{\beta},\tilde{\sigma}^2_{Q,s},\tilde{\sigma}^2_{P,s})} \boldsymbol{D}\boldsymbol{W}^{-1}\boldsymbol{D}', \tag{64}$$

where the moment vector $\boldsymbol{D}$ is defined as:

$$\boldsymbol{D} = \begin{pmatrix} \mathrm{Vech}(\hat{\boldsymbol{\Sigma}}_1 - \hat{\boldsymbol{\Sigma}}_0) - \mathrm{Vech}(\boldsymbol{\alpha}\boldsymbol{\alpha}' + \boldsymbol{\beta}\boldsymbol{\beta}'\tilde{\sigma}^2_{P,s}) \\ \mathrm{Vech}(\hat{\boldsymbol{\Sigma}}_2 - \hat{\boldsymbol{\Sigma}}_0) - \mathrm{Vech}(\boldsymbol{\alpha}\boldsymbol{\alpha}'\tilde{\sigma}^2_{Q,s} + \boldsymbol{\beta}\boldsymbol{\beta}') \end{pmatrix}. \tag{65}$$

Here, $\hat{\boldsymbol{\Sigma}}_i$ (for $i = 0, 1, 2$) is the sample variance-covariance matrix of the VAR residuals for days in Event i (Event 0: non-announcement days; Event 1: Q-announcement days; Event 2: P-announcement days). The operator Vech$(\cdot)$ vectorizes the lower triangular part of a symmetric matrix, ensuring we use only independent moment conditions.

$\boldsymbol{W}$ is the GMM weighting matrix, which we specify as a diagonal matrix to simplify the optimization given the high dimensionality of our problem ($n \times (n+1)$ moment conditions for n bond yields):

$$\boldsymbol{W} = \begin{pmatrix} diag(\hat{\boldsymbol{V}}_0 + \hat{\boldsymbol{V}}_1) & \mathbf{0} \\ \mathbf{0} & diag(\hat{\boldsymbol{V}}_0 + \hat{\boldsymbol{V}}_2) \end{pmatrix}, \tag{66}$$

where $\hat{\boldsymbol{V}}_i$ denotes the estimated variance-covariance matrix of Vech$(\hat{\boldsymbol{\Sigma}}_i)$. This construction follows Wright (2012) but uses a diagonalized weighting matrix for computational tractability. For statistical inference, we implement the stationary bootstrap proposed by Politis and Romano (1994) to address potential volatility clustering in yield residuals. We set the expected block length to 10 trading days, a choice balanced to capture short-term dynamics in bond markets without over-smoothing. This bootstrap procedure generates robust confidence intervals for all parameter estimates.

3.6 Comparison with Other Heteroskedasticity Settings

Our ordered-heteroskedasticity framework not only identifies dual shocks but also provides a natural solution to the labeling problem by assigning clear economic interpretations. This section clarifies the methodological distinctions between our approach and other established heteroskedasticity-based identification strategies.

Our setting diverges from Lanne et al. (2010) in two fundamental aspects, as their framework considers Markov-switching volatility regimes. First, while both methods leverage variance regimes, the economic intuition differs substantially. Lanne et al. (2010) identify shocks based on the relative variance of different shocks within the same regime. In contrast, our identification rests on the variance ordering for a single shock across different events/regimes, which directly reflects the difference in information content between loud and silent news. Second, by imposing this intuitive ordering, we not only achieve identification but also economically label the shocks as quantity-target and price-target shocks—a step that remains an *ex-post* challenge in their multi-regime models.

Our strategy also differs from the integrated approach of Gürkaynak et al. (2020), who combine OLS and heteroskedasticity to identify non-headline news. Their methodology can be formalized as:

$$y_t = \boldsymbol{\beta}' s_t + \gamma' d_t f_t + \epsilon_t. \tag{67}$$

Crucially, it depends on the observability of the headline news s_t (e.g., from federal funds futures). The heteroskedasticity assumption is then applied to the residual to identify the unobserved non-headline shock f_t. This approach is infeasible in China due to the absence of suitable derivatives to directly observe any policy target shock. Our model, by contrast, uses heteroskedasticity alone to simultaneously identify both the loud- and silent-news shocks, relaxing the stringent requirement for an observable proxy.

Finally, our framework is general and nests several simpler specifications as special cases. By tightening the constraints in Equations (5) and (6), we can derive alternative models:

- **Single-Shock Specification:** By imposing the constraints $\sigma^2_{Q,s} = \sigma^2_{Q,0}$ and $\sigma^2_{P,s} = \sigma^2_{P,0}$, we effectively assume the absence of silent news shock. This reduces the moment conditions to:

$$\Delta\boldsymbol{\Sigma}_1 = \boldsymbol{\alpha}\boldsymbol{\alpha}', \tag{68}$$

$$\Delta\boldsymbol{\Sigma}_2 = \boldsymbol{\beta}\boldsymbol{\beta}'. \tag{69}$$

  Under these conditions, the abnormal yield variation on announcement days is attributed to a single shock for each announcement type, as employed in Lin and Niu (2021).

- **Undifferentiated Shock Specification:** A further simplification assumes $\boldsymbol{\alpha} = \boldsymbol{\beta}$, implying that different announcements induce identical yield curve impacts. This leads to a three-regime model where a single shock's variance differs across announcement types, a specification also explored in Lin and Niu (2021) to compare the magnitude of announcement effects.

- **Basic Two-Regime Specification:** The most simplified case further assumes $\sigma^2_{Q,l} = \sigma^2_{P,l}$, treating all announcements as equivalent and eschewing any distinction between the shocks they cause. This results in the standard two-regime heteroskedastic model used in studies such as Wright (2012), Bu et al. (2021) and Lin and Niu (2021).

Our dual-shock specification offers a more nuanced and empirically superior representation, as demonstrated in subsequent sections, by capturing the multifaceted information content of policy announcements within China's dual-target framework.

4 Data

This section describes the two core datasets used in our empirical analysis: monetary policy announcements and interest rates. We first detail the collection and classification of PBoC policy announcements, which constitute the events central to our identification strategy. Subsequently, we present the interest rate data—Treasury bond yields and interbank offered rates—which serve as the financial market variables whose responses to the identified shocks are analyzed. The sample period spans from October 8, 2006, to December 31, 2022.

4.1 Monetary Policy Announcements

This subsection details the definition, sample selection, and event window construction for monetary policy announcements, which form the foundation for the subsequent identification and estimation.

4.1.1 Classification of Announcement Types

We classify monetary policy announcements by the PBoC into two categories, aligning with China's dual-target operational framework:

- **Q-announcements:** Adjustments to the RRR, a core quantitative tool for managing banking system liquidity and broad money supply.
- **P-announcements:** Adjustments to key price-target-based policy rates. This includes adjustments to the BLDR and, following the reform of the Loan Prime Rate (LPR) formation mechanism, adjustments to the MLF rate.

4.1.2 Sample Period and Policy Regime Considerations

Our sample begins on October 8, 2006, which coincides with the launch of the Shanghai Interbank Offered Rate (Shibor). This date marks the start of a consistent, market-based benchmark for short-term interbank funding costs in China—a necessary condition for analyzing monetary policy transmission to money markets. From this point, we trace the evolution of the PBoC's operational framework.

Our classification of price-target announcements reflects an important policy evolution during the sample period. Prior to the LPR reform on August 17, 2019, the BLDR served as the primary benchmark for bank lending. After the reform, the MLF rate became the de facto anchor for medium-term policy rates, as the LPR is quoted by commercial banks as the MLF rate plus a spread.

In parallel, the PBoC began cultivating a new short-term policy rate anchor. Official communications progressively signaled this shift. The *China Monetary Policy Execution Report* of the Fourth Quarter of 2020 explicitly identified the 7-day reverse repo rate as a key policy rate for assessing short-term interest rate trends.[6] Further evidence emerged in the report released on August 17, 2023: while its summary listed both the MLF and reverse repo rates as policy rates, the main text, when detailing how to guide market interest rates lower, mentioned *only* the reduction in the 7-day reverse repo rate.[7] This nuanced phrasing indicated the central bank's intent to elevate this rate's role within the framework. A decisive signal came on June 19, 2024, when PBoC Governor Gongsheng Pan stated at the 15th Lujiazui Forum that the 7-day reverse repo rate had essentially assumed the function of the primary policy rate.

This ongoing shift of the policy anchor from medium- to short-term rates introduces a potential structural break. To maintain a consistent definition of the price target and ensure the stability of the transmission mechanism we aim to identify, we conclude our sample on December 31, 2022. This endpoint allows us to analyze a period in which the BLDR and MLF rates served as a clear and stable medium-term anchor, prior to the heightened emphasis on the short-term reverse repo rate became pronounced in subsequent communications and actions.

Based on the above consideration, we collect all PBoC announcements on RRR, BLDR, and MLF rate adjustments from October 8, 2006, through December 31, 2022. We exclude eight announcements involving simultaneous adjustments to both RRR and BLDR. This exclusion is justified on two grounds: first, separate single-instrument adjustments provide sufficient moment conditions for identifying distinct quantity- and price-target shocks; second, modeling simultaneous adjustments would require specifying an additional variance regime,

[6] Available at https://www.pbc.gov.cn/zhengcehuobisi/125207/125227/125957/4021036/8d39aa9d730046c896289d17c09346d2/2021020821282167078.pdf

[7] Available at https://www.pbc.gov.cn/zhengcehuobisi/125207/125227/125957/4883187/e6dc129d48d9474cb6455691eee05766/2023081717054357626.pdf

but the scant number of such joint events (only 8) is insufficient for reliably estimating the necessary variance-covariance matrix. After this exclusion, our final sample comprises:

- 43 Q-announcements (RRR adjustments only);
- 21 P-announcements (16 BLDR adjustments and 5 MLF rate adjustments).

4.1.3 Event Windows for Shock Measurement

To capture market innovations induced by monetary policy announcements, we define the measurement timing based on each announcement's specific release time. The general principle is to use the innovation from the first subsequent trading day for announcements issued after market close or on holidays, which constitute the vast majority of cases. For intraday announcements, we typically use the innovation from the announcement day itself.

A crucial exception to this rule is the RRR hike announced on June 14, 2011, at 15:18:25. Despite its intraday release, the Treasury yield curve moved only marginally on that day (e.g., the 3-month yield rose a mere 5 basis points). In stark contrast, the 3-month yield surged by 18 basis points on the following trading day. Contemporary news reports uniformly attributed this turmoil to the announcement.[8] Consequently, we employ the innovation from the *second* trading day to better gauge this announcement's impact.

Finally, for non-announcement days, we define the 10 trading days preceding each announcement as the non-announcement window. This accounts for potential volatility clustering in the residuals and provides a stable baseline for estimating the variance-covariance matrices required for identification. Detailed announcement dates and times are provided in Appendix Table A.1.

4.2 Interest Rate

Our empirical analysis employs two complementary sets of interest rate data over the sample period defined in Section 4.1.2 (October 8, 2006, to December 31, 2022): Treasury bond yields, which serve as the primary variables for identifying monetary policy shocks; and Shanghai Interbank Offered Rate (Shibor), which allow us to examine the transmission of

[8] A *Securities Times* report (available at https://www.cei.cn/defaultsite/s/article/2011/06/15/4b4ff4a5-3a0ff4b0-013a-10321d53-5b96_2011.html?columnId=4028c7ca-37115425-0137-115c2371-10e6&referCode=fnywzs) explains the delayed spot market reaction, noting that "the central bank announcing a major monetary policy during trading hours was, in memory, the first time in recent years, leaving everyone somewhat at a loss," and that subsequently "fund lending became difficult as lenders withdrew their quotes en masse." This suggests the unconventional timing triggered panic and an instantaneous liquidity dry-up, temporarily crippling price discovery.

shocks to the money market. All data are sourced from Wind Info, a leading Chinese financial data provider.

4.2.1 Treasury Bond Yields

To identify the monetary policy shocks, we use zero-coupon yields on Chinese Treasury bonds compiled by China Central Depository & Clearing Co., Ltd. (CCDC). The selected eight maturities are 3 months, 6 months, 9 months, 1 year, 3 years, 5 years, 7 years, and 10 years, providing comprehensive coverage of the yield curve from the short to the long end. Figures 2 illustrates the evolution of these yields over the sample period.

4.2.2 Shibor Rates

To further investigate the effects of the identified shocks on money-market conditions, we employ the Shibor. Shibor is a key daily reference rate in China's interbank market, calculated from quotes submitted by eighteen major commercial banks. We use all eight published tenors: overnight (O/N), 1 week, 2 weeks, 1 month, 3 months, 6 months, 9 months, and 1 year. Figures 3 plots the time series of Shibor rates across these maturities.

5 Empirical Results

This section presents the core empirical findings. We first report and interpret the estimated structural parameters, which reveal distinct transmission channels for quantity-target versus price-target shocks and quantify the informational role of silent news. We then evaluate model performance by examining the identified shock series and their explanatory power for yield innovations. Finally, we establish economic significance by showing that silent news predicts future policy adjustments and that all shocks trigger persistent responses in both bond yields and money market rates.

5.1 Parameter Estimates

5.1.1 Impact Coefficients of the Dual Shocks

Table 2 presents the estimated impact coefficients of the identified structural shocks across the yield curve. The results reveal distinct transmission channels. Under the dual-shock specification, Q-target shocks exhibit a stronger influence on short-term yields, with statistical significance at the 1% level for all maturities. In contrast, P-target shocks have a statistically

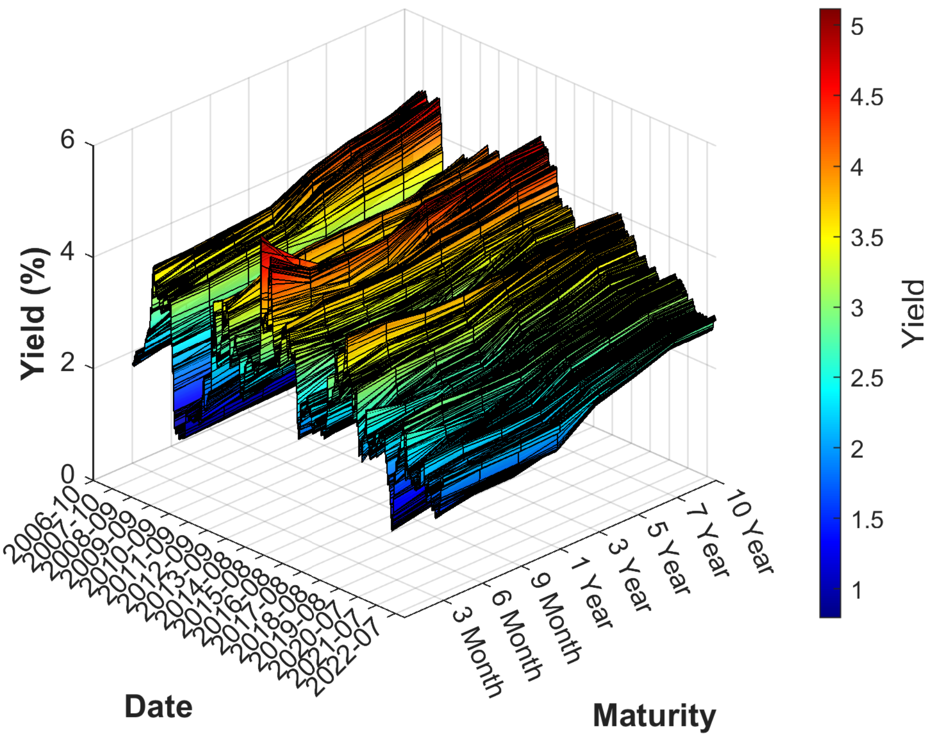

Figure 2: Daily Time Series of Zero-coupon Yields

Note: This figure plots the daily time series of zero-coupon yields on Chinese Treasury bonds across eight maturities (3-month, 6-month, 9-month, 1-year, 3-year, 5-year, 7-year, and 10-year). The data span from October 8, 2006, to December 31, 2022. Zero-coupon yields are compiled by China Central Depository & Clearing Co., Ltd. (CCDC) and sourced from Wind Info.

insignificant impact on the 3-month yield but exert a significant and growing influence on yields of 6-month maturity and longer.

This term structure of the impact coefficients aligns with the behavior of major market participants. Commercial banks, the dominant holders of Treasury bonds in China, tend to be patient fixed-income investors (Hanson et al., 2015). When reserve requirement adjustments reduce excess reserves, banks are more likely to rebalance portfolios by adjusting holdings of liquid short-term bonds, exerting greater pressure on short-term yields. Conversely, the increasing impact of P-target shocks with maturity is consistent with the Preferred-Habitat hypothesis (Vayanos and Vila, 2021). As Treasury bonds and bank loans are substitutes, a rise in benchmark lending rates reduces loan attractiveness, increasing bank demand for bonds, particularly in the long end where they have a preferred habitat, thus pushing long-

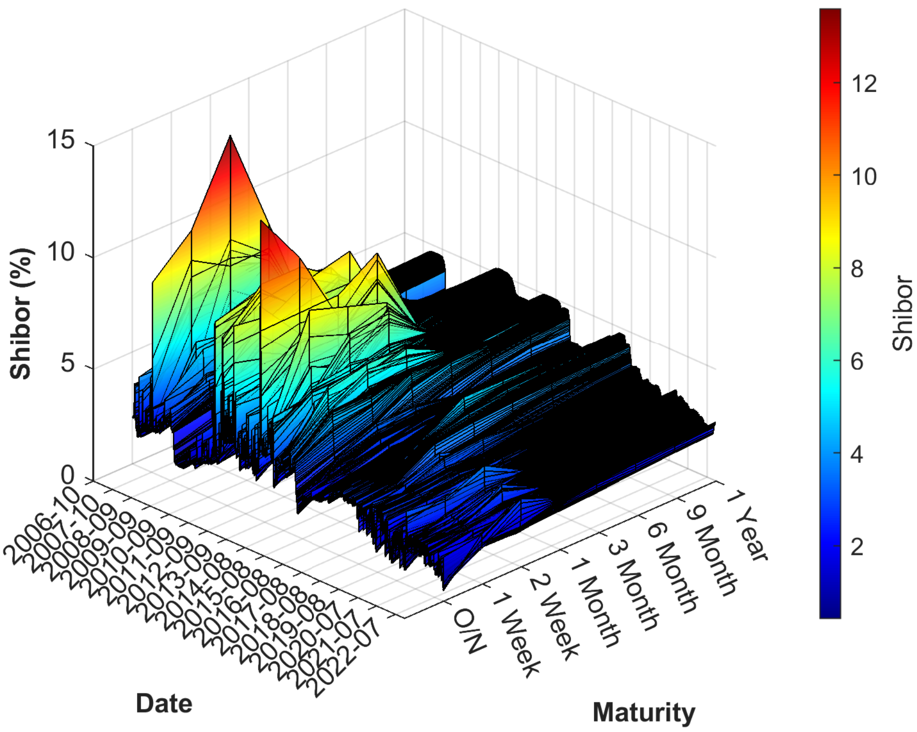

Figure 3: Daily Time Series of Shibor Rates

Note: This figure plots the daily time series of the Shanghai Interbank Offered Rate (Shibor) across eight maturities (O/N, 1-week, 2-week, 1-month, 3-month, 6-month, 9-month, and 1-year). The data span from October 8, 2006, when Shibor was officially launched, to December 31, 2022. Shibor rates are sourced from Wind Info.

term yields down more strongly.

Notably, the pattern of amplified impacts of P-target shocks on longer-maturity bonds runs counter to the traditional Expectations Hypothesis and stands in contrast to findings on U.S. monetary policy target shocks (Gürkaynak et al., 2005), where policy shocks exert a dominant influence on short-term interest rates. This divergence stems from a key distinction in policy transmission mechanisms: unlike the U.S. framework, where shocks propagate from the ultra-short-term federal funds rate, the PBoC's price-target-based tools in our sample period are explicitly designed to directly anchor banks' medium- to long-term deposit and lending rates. As a result, adjustments to the price target are transmitted to short-term interest rates with a discernible time lag. Evidence to support this argument with lagged short-term Shibor responses will be presented in Section 5.5.

A comparison with the single-shock specification underscores the dual-shock model's ad-

Table 2: Impact Coefficients of Identified Shocks

Maturity	Q-Target Shock Impact: $\boldsymbol{\alpha}$		P-Target Shock Impact: $\boldsymbol{\beta}$	
	Dual-Shock	Single-Shock	Dual-Shock	Single-Shock
3M	0.0578***	0.0599***	0.0154	0.0157
	[0.0214,0.0887]	[0.0229,0.0858]	[-0.0112,0.0450]	[-0.0144,0.0446]
6M	0.0616***	0.0676***	0.0248*	0.0249*
	[0.0315,0.0926]	[0.0347,0.0917]	[-0.0001,0.0583]	[-0.0039,0.0564]
9M	0.0626***	0.0677***	0.0450**	0.0452*
	[0.0297,0.0913]	[0.0332,0.0927]	[0.0088,0.0817]	[-0.0016,0.0809]
1Y	0.0603***	0.0653***	0.0536**	0.0536*
	[0.0310,0.0855]	[0.0340,0.0882]	[0.0200,0.0775]	[-0.0094,0.0773]
3Y	0.0318***	0.0427***	0.0539**	0.0541*
	[0.0158,0.0496]	[0.0218,0.0544]	[0.0201,0.0828]	[-0.0116,0.0822]
5Y	0.0358***	0.0459***	0.0685**	0.0681*
	[0.0154,0.0574]	[0.0217,0.0618]	[0.0310,0.0962]	[-0.0308,0.0955]
7Y	0.0221***	0.0327***	0.0755**	0.0751*
	[0.0070,0.0421]	[0.0127,0.0463]	[0.0241,0.1102]	[-0.0264,0.1105]
10Y	0.0267***	0.0366***	0.0690**	0.0693*
	[0.0093,0.0467]	[0.0147,0.0510]	[0.0238,0.0980]	[-0.0179,0.0982]

Note: $\boldsymbol{\alpha}$ represents the impact coefficient of quantity-target shocks, and $\boldsymbol{\beta}$ represents the impact coefficient of price-target shocks; The square brackets show the 2.5% and 97.5% sampling quantiles obtained from bootstrap with 20,000 replications. The symbols ***, *, and * represent significance at the 1%, 5%, and 10% levels, respectively.

vantages. The estimated coefficients for Q-target shocks differ notably between specifications, especially at longer maturities, suggesting the single-shock model inaccurately absorbs effects from silent P-target shocks. While point estimates for P-target shocks are similar, the dual-shock specification yields estimates with higher statistical significance, demonstrating enhanced efficiency from explicitly modeling silent news.

5.1.2 Heteroskedasticity in Shock Variances

The heteroskedasticity parameters quantify the informational content of silent news and reveal important differences between announcement types. Panel A of Table 3 reports the variance jumps for silent news. The results show a striking asymmetry: the variance jump for Q-target shocks on P-announcement days ($\tilde{\sigma}^2_{Q,s}$) is negligible, while that for P-target shocks on Q-announcement days ($\tilde{\sigma}^2_{P,s}$) is substantial.

This pattern is corroborated by the estimated shock variances across event types in Panel B. The variance of the Q-target shocks during P-announcements (0.3253) is virtually indistinguishable from its variance on non-announcement days (0.3198). In contrast, the variance of the P-target shocks on Q-announcement days (0.2483) is approximately double that on non-announcement days (0.1209), confirming that a substantial portion of yield volatility on Q-announcement days originates from silent news about price targets.

Table 3: Heteroskedasticity in Variance

Panel A: Variance Jumps		
Parameter	Interpretation	Estimate
$\tilde{\sigma}^2_{Q,s}$	Variance jump of Q-target shock on P-announcement vs. non-announcement	1.0366×10^{-5} $[3.6236\times10^{-8}, 0.0003]$
$\tilde{\sigma}^2_{P,s}$	Variance jump of P-target shock on Q-announcement vs. non-announcement	0.1155 $[1.1132\times10^{-8}, 0.4987]$
Panel B: Variances of Shocks on Announcement and Non-announcement Days		
Event Type	Q-Target Shock	P-Target Shock
Q-announcement	1.3537	0.2483
	[0.7160,1.3968]	[0.0573,0.5259]
P-announcement	0.3253	0.9690
	[0.0075,0.4817]	[0.1901,1.1502]
Non-announcement	0.3198	0.1209
	[0.0823,0.4493]	[0.0450,0.3199]

Note: This table presents parameter estimates characterizing shock heteroskedasticity. Panel A reports the estimated variance jumps. Specifically, $\tilde{\sigma}^2_{P,s}$ measures the change in the variance of price-target (P-target) shocks on quantity-target announcement days (Q-announcement) relative to non-announcement days. Conversely, $\tilde{\sigma}^2_{Q,s}$ measures the change in the variance of quantity-target (Q-target) shocks on price-target announcement days (P-announcement) relative to non-announcement days. Panel B displays the variances of both Q-target and P-target shocks on Q-announcement, P-announcement, and non-announcement days, computed using Equation (51). The values in brackets represent the 2.5% and 97.5% bootstrap quantiles.

This asymmetry in informational content stems directly from the PBoC's operational framework and the resulting information environment for market participants. The central bank employs quantity tools, particularly RRR adjustments, more frequently and supports them with routine open market operations that provide high-frequency liquidity signals. This steady flow of information enables investors to form relatively precise expectations about the quantity-policy stance. Consequently, when a price-target-based announcement occurs, it offers little incremental information regarding quantity targets, resulting in nearly homoskedastic silent Q-target shocks. In contrast, adjustments to price-target-based tools are less frequent and are not preceded by comparable daily signals, leaving market expectations about the price target more diffuse. A quantity announcement therefore conveys substantial incremental information about the future trajectory of price policy, generating the significant heteroskedasticity observed for silent P-target shocks.

The economic implications directly inform model comparison. The negligible $\tilde{\sigma}^2_{Q,s}$ explains why the single-shock specification yields similar estimates for P-target shocks—it approximates the correct model for P-announcements. However, for Q-announcements, the single-shock model is misspecified, forcing the Q-target shocks to explain variation actually caused by volatile silent P-target shocks. This contamination explains discrepancies in Q-target impact coefficients and confirms the dual-shock framework's superior identification.

5.2 Time Series of Shocks and Goodness of Fit

Having identified the structural parameters, we now examine the time series of the identified announcement-induced shocks and evaluate the ability of the dual-shock specification to explain yield innovations. This analysis serves two purposes: to validate the economic intuition behind the identified shocks, and to quantitatively compare the performance of our model against the traditional single-shock specification.

5.2.1 Time Series Properties of Structural Shocks

We compute the shock series for each announcement following *Proposition* 2. The results are plotted in Figure 4. Each announcement generates two shocks: one from the loud news and another from the silent news. For Q-announcements, we label the quantity-target shocks induced by the loud news as the *Q-target L* shock, and the price-target shocks induced by silent news as the *P-target S* shock. Analogously, for P-announcements we obtain *P-target L* shocks and *Q-target S* shocks. For comparison, Figure 4 also includes the shocks estimated under the single-shock specification.

Consistent with our identification assumptions, Q-announcements are dominated by *Q-target L* shocks, while P-announcements are dominated by *P-target L* shocks, as evidenced by their larger absolute magnitudes in Figure 4. The dominant shocks in the dual-shock specification are highly correlated with their counterparts in the single-shock specification (approximately 0.93 for Q-announcements and 0.99 for P-announcements). This indicates that the single-shock model, though misspecified, still captures the primary loud-news component of the announcements. The silent-news shocks, which the single-shock specification ignores, sometimes align with and other times oppose the direction of the loud-news shocks. This reflects the complex nature of market expectation adjustments, where investors may perceive policy

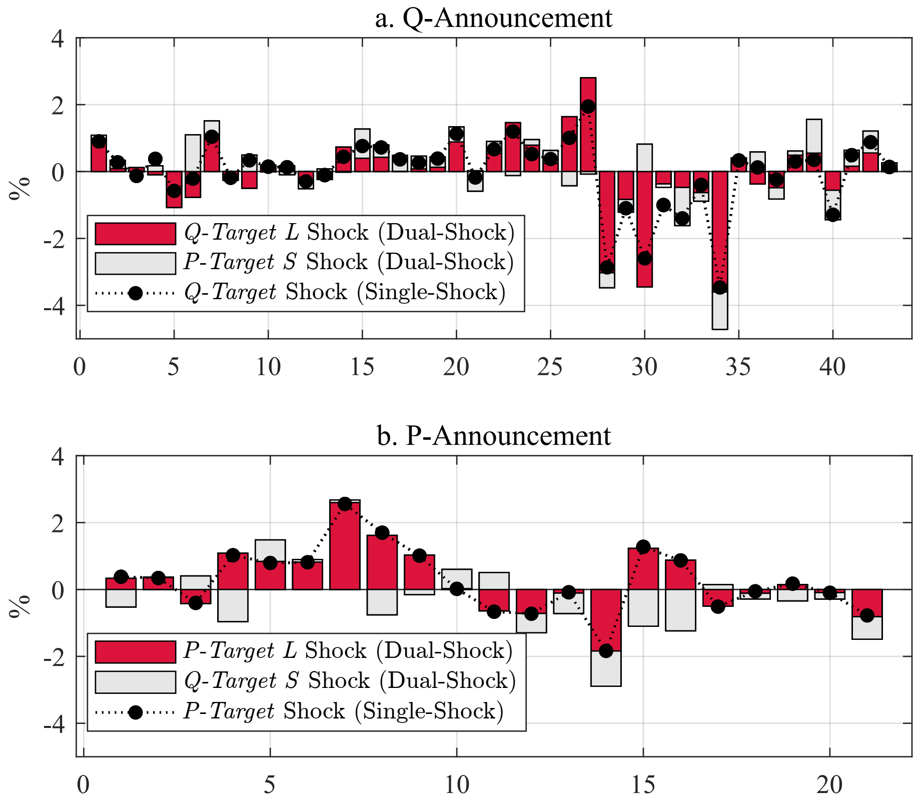

Figure 4: Shock Series

Note: This figure displays the time series of estimated structural shocks. Q-announcement and P-announcement denote quantity-target-based and price-target-based announcements by the PBoC, respectively. For Q-announcements, the quantity-target shocks from loud news are labeled *Q-target L*, and the price-target shocks from silent news are labeled *P-target S*. For P-announcements, the price-target shocks from loud news are labeled *P-target L*, and the quantity-target shocks from silent news are labeled *Q-target S*. For comparison, the figure also includes shocks identified under the single-shock specification, where the shocks extracted from a Q-announcement are labeled *Q-target*, and from a P-announcement are labeled *P-target*.

tools as either complementary or substitutable following a central bank signal.

5.2.2 Goodness of Fit

To formally evaluate model performance, we compare the goodness-of-fit of the dual-shock and single-shock specifications. Figures 5 and 6 plot the adjusted R-squared values obtained from regressing the identified shocks onto the VAR residuals for Q-announcement and P-announcement days, respectively.

On Q-announcement days (Figure 5), the *Q-target L* shocks driven by loud news provide the strongest explanation for short- to medium-term yield innovations, with adjusted R-squared values peaking at 90% for the 1-year yield. The *P-target S* shocks carried by silent

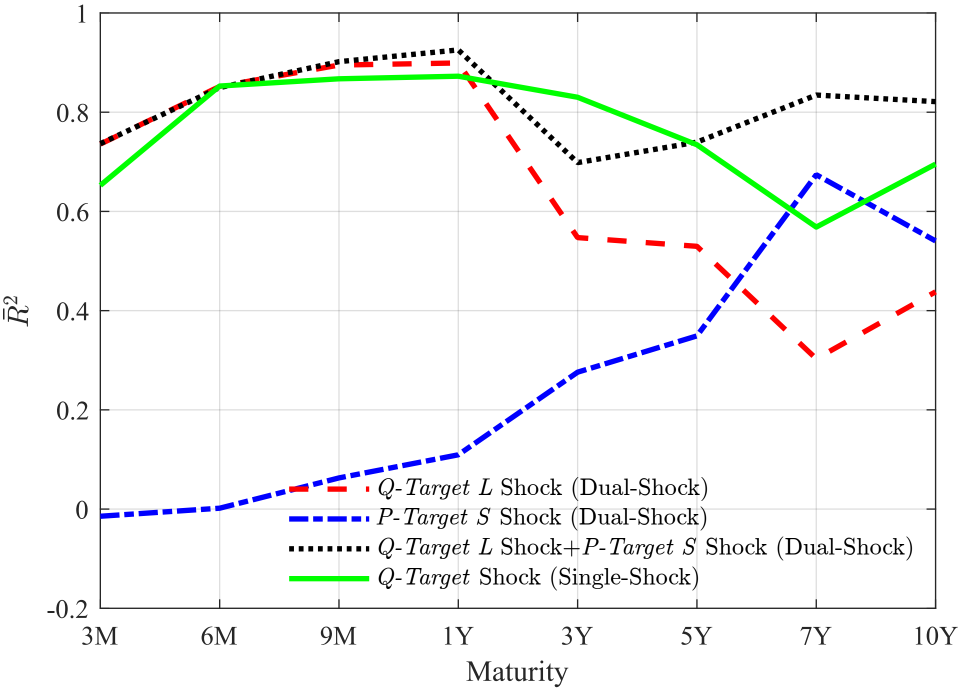

Figure 5: Comparison of Adjusted R-squared Values for Q-announcements

Note: This figure presents the adjusted R-squared values from regressing the identified shocks on the VAR residuals for the 43 Q-announcement days in our sample. Q-announcements denote the PBoC's quantity-target-based policy announcements. It compares the explanatory power of the dual-shock and single-shock specifications. In the dual-shock specification, the *Q-target L* shock refers to the quantity-target shock from loud news, while the *P-target S* shock refers to the price-target shock from silent news. In the single-shock specification, the *Q-target* shock is the sole shock identified from Q-announcements.

news, in contrast, exhibit negligible explanatory power for short-term yields but becomes increasingly important for longer maturities, explaining up to 68% of the variation in the 7-year yield. The combined term determined by both shocks consistently outperforms the single-shock specification across almost the entire yield curve, demonstrating that silent price news provides significant incremental explanatory power.

On P-announcement days (Figure 6), the *P-target L* shocks driven by loud news effectively explain medium- to long-term yield movements. The *Q-target S* shocks carried by silent news complement this by adding explanatory power for short-term yields. Consequently, the dual-shock specification achieves a superior overall fit compared to the single-shock model, which captures only the loud-news effect. This complementary pattern underscores that both types of announcements contain multidimensional information that affects different segments of the yield curve.

In sum, the dual-shock specification demonstrates a systematically superior capacity to capture yield innovations. The incorporation of silent news shocks, which the single-shock

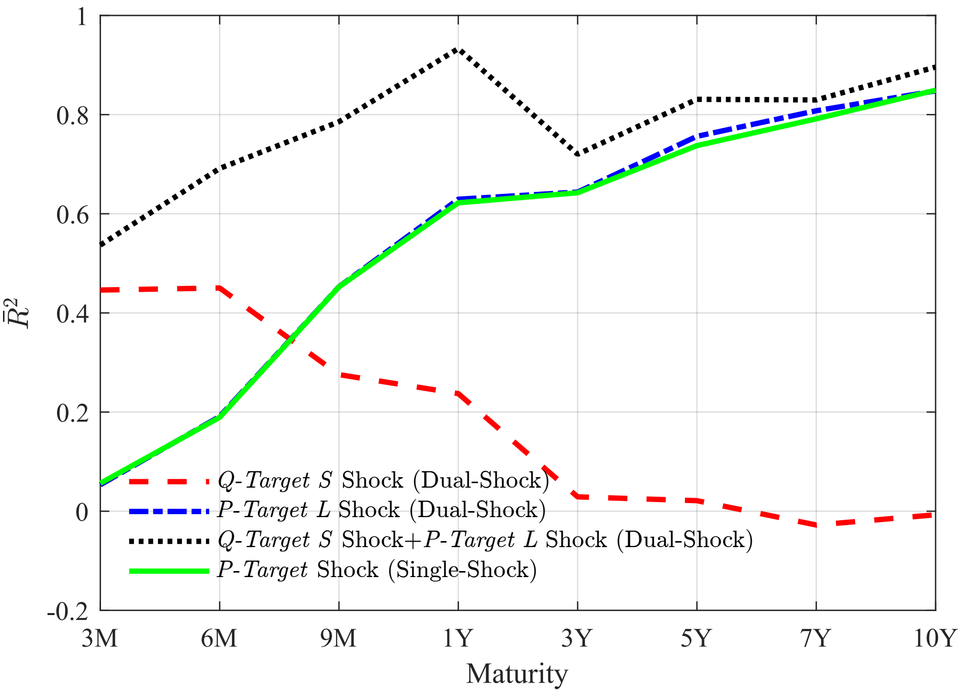

Figure 6: Comparison of Adjusted R-squared Values for P-announcements

Note: This figure presents the adjusted R-squared values from regressing the identified shocks on the VAR residuals for the 21 P-announcement days in our sample. P-announcements denote the PBoC's price-target-based policy announcements. It compares the explanatory power of the dual-shock and single-shock specifications. In the dual-shock specification, the *P-target L* shock refers to the price-target shock from loud news, while the *Q-target S* shock refers to the quantity-target shock from silent news. In the single-shock specification, the *P-target* shock is the sole shock identified from P-announcements.

model omits, provides significant additional explanatory power, validating our core premise that China's monetary policy announcements contain and transmit dual-dimensional information.

5.3 The Economic Significance of Silent-News Shocks

The superior goodness-of-fit of the dual-shock specification raises a valid question: are the identified silent-news shocks merely a statistical artifact that overfits the data, or do they contain genuine economic information? To address this concern, we test a central economic implication of our framework: if silent-news shocks accurately reflect the market's updating of expectations for non-announced policy targets, then these shocks should help predict the central bank's future policy actions.

Our identification strategy inherently links silent news to the PBoC's policy coordination. While loud-news shocks capture the direct surprise of the announced target (e.g., an unexpected RRR cut), silent-news shocks represent the market's inference about the implicit target based on that announcement (e.g., revising the expectation for future interest rates following an RRR cut). If markets are efficient and understand the central bank's reaction function, these inferred adjustments should foreshadow actual future policy changes.

To test this hypothesis, we examine whether cumulative silent-news shocks predict subsequent changes in the PBoC's policy targets. We estimate the following regression model separately for price and quantity targets:

$$\Delta\text{Target}_i = \gamma_0 + \gamma_1 \sum_{j \in \Theta_i} \text{Silent\_target}_j + \epsilon_i. \tag{70}$$

Here, ΔTarget_i is the actual target adjustment by the PBoC in the i^{th} announcement of a given type. The key explanatory variable, $\sum_{j\in\Theta_i} \text{Silent\_target}_j$, is the cumulative sum of the relevant silent-news shocks that occurred between the i^{th} and $(i-1)^{\text{th}}$ announcements of that target type in between, where Θ_i denotes the set of intervening announcements of the other type. For example, for a price-target change, we accumulate the *P-target S* shocks from all Q-announcements that occurred since the last price change. Because not every policy announcement is preceded by an alternative-type announcement, our final sample consists of 18 observations for price-target regressions and 18 for quantity-target regressions.

Table 4: Predictive Power of Cumulative Silent News for Policy Adjustments

	$\sum_{j\in\Theta_i} \text{Silent\_target}_j$	Adj. $\bar{R}^2$	No. Obs
Price Target Change	0.1316* (0.0786)	0.0957	18
Quantity Target Change	0.2296 (0.2034)	0.0159	18

Note: This table presents the results from regressions $\Delta\text{Target}_i = \gamma_0 + \gamma_1 \sum_{j\in\Theta_i} \text{Silent\_target}_j + \epsilon_i$, where ΔTarget_i denotes PBoC's announced adjustment to its target, $\sum_{j\in\Theta_i} \text{Silent\_target}_j$ captures the cumulative silent news shocks between the i^{th} and $i-1^{th}$ announcements where Θ_i denotes the set of announcements released during this interval. The second row and third row provides the results of regressions on price target and quantity target respectively. Standard errors are in parentheses. The symbols ***, *, and * represent significance at the 1%, 5%, and 10% levels, respectively.

The regression results, presented in Table 4, provide clear evidence for the economic significance of silent news, particularly regarding price targets. The cumulative *P-target S* shocks are a statistically significant predictor of future price-target adjustments. The positive coefficient indicates that when markets infer a tighter (easier) price stance from a series of Q-announcements, the PBoC is subsequently more likely to raise (cut) its price targets. This silent-news channel serves as potent forward guidance, with the cumulative shocks explaining about 10% of the variation in future price-target changes.

In contrast, the cumulative *Q-target S* shocks show a positive but statistically insignificant relationship with future quantity adjustments. This asymmetry is consistent with the heteroskedasticity patterns documented in Table 3. The PBoC's frequent use of quantity tools and open market operations provides markets with ample direct information, reducing the need to infer quantity targets from price announcements. Consequently, the *Q-target S* shocks are less volatile and less predictive of actual policy.

These findings robustly refute the notion that silent-news shocks are merely statistical overfitting. Instead, they represent economically meaningful updates to market expectations that contain valuable forward-looking information about the PBoC's policy trajectory, especially concerning future price settings. This evidence solidifies the economic interpretation of our identified shocks and underscores the importance of decoding the implicit signals embedded in China's monetary policy announcements.

5.4 Dynamic Effects of Shocks on Treasury Bond Yields

To move beyond the immediate impact and examine the full dynamic tranmission of shocks through the bond market, we estimate the persistent effects of all four identified shocks on Treasury bond yields. We employ the local projection method to trace impulse responses over a horizon of h trading days, using the following specification:

$$y_{t+h} = \upsilon_h + \rho_h Shock_t + \varphi_h y_{t-1} + \psi_h \tilde{F}_t + \epsilon_{t+h}, \ h = 0, 1, 2, \cdots, n, \cdots . \tag{71}$$

Here, y_t denotes the Treasury bond yield, and $Shock_t$ represents the shock series whose dynamic effect is being traced. On non-announcement days, $Shock_t$ is set to zero; on announcement days, it equals the value of the corresponding shock identified in our model. In constructing the loud news shock series, we incorporate shocks from the rare announcements of simultaneous RRR and BDLR adjustments (excluded from the main identification) to better capture the effects of these joint policy actions, which convey loud news for both targets. We treat both shocks as driven by loud news on such simultaneous announcements days and derive shock values using the estimated impact coefficients at the 3-month, 1-year, and 10-year maturities from Table 2, together with the corresponding VAR residuals.[9] The vector of control variables $\tilde{F}_t$ includes all other identified policy shocks (both loud and silent)

[9]Due to the limited sample of only 8 simultaneous RRR and BDLR announcements (Section 4.1.2), we cannot precisely estimate the 8×8 variance-covariance matrix required for shock identification. We therefore identify the shocks using a parsimonious set of three yields spanning the short-, medium-, and long-term segments of the curve.

to isolate the effect of the shock of interest. This specification yields the impulse-response coefficient $\hat{\rho}_h$ for each horizon h.

5.4.1 Responses to Loud-News Shocks

Figures 7 and 8 plot the estimated impulse responses of yields to the loud-news shocks, along with 95% confidence bands.

Q-target L Shocks (Figure 7) exert an immediate effect on short-term yields. Their influence on medium- and long-term yields is also significant but weakens as maturity increases.

P-target L Shocks (Figure 8) produce a notably delayed response in short-term yields, which become significant only after a lag. Once the effect materializes, it is larger and more persistent than that of quantity shocks. The impact on medium- and long-term yields is more immediate but gradually diminishes with maturity. Overall, *P-target L* shocks exert stronger and more enduring effects on the medium to long end of the yield curve compared to *Q-target L* shocks.

5.4.2 Responses to Silent-News Shocks

Figures 9 and 10 present the analogous results for silent-news shocks. These reveal that the silent-news shocks, though smaller in initial variance, also generate statistically significant dynamic effects.

Q-target S shocks (Figure 9) exert an immediate, though short-lived, influence, with a more notable impact on short-term yields that persists for up to about 20 trading days.

P-target S shocks (Figure 10) show a distinctly lagged response pattern. Yields with maturities below one year respond significantly around 210 trading days after the shock, while yields above five years exhibit a pronounced and highly persistent response beginning around 150 trading days post-shock. This delayed but powerful effect is consistent with silent news containing forward guidance about the future policy stance.

5.4.3 Summary of Dynamic Effects

The dynamic analysis reveals a complex tapestry of effects. Loud-news shocks trigger immediate and persistent adjustments, with *Q-target L* shocks displaying a delayed but powerful influence on short-term rates. Crucially, silent-news shocks are not transient; they contain meaningful information that manifests in significant dynamic responses across the yield curve, underscoring their role in the monetary policy transmission mechanism.

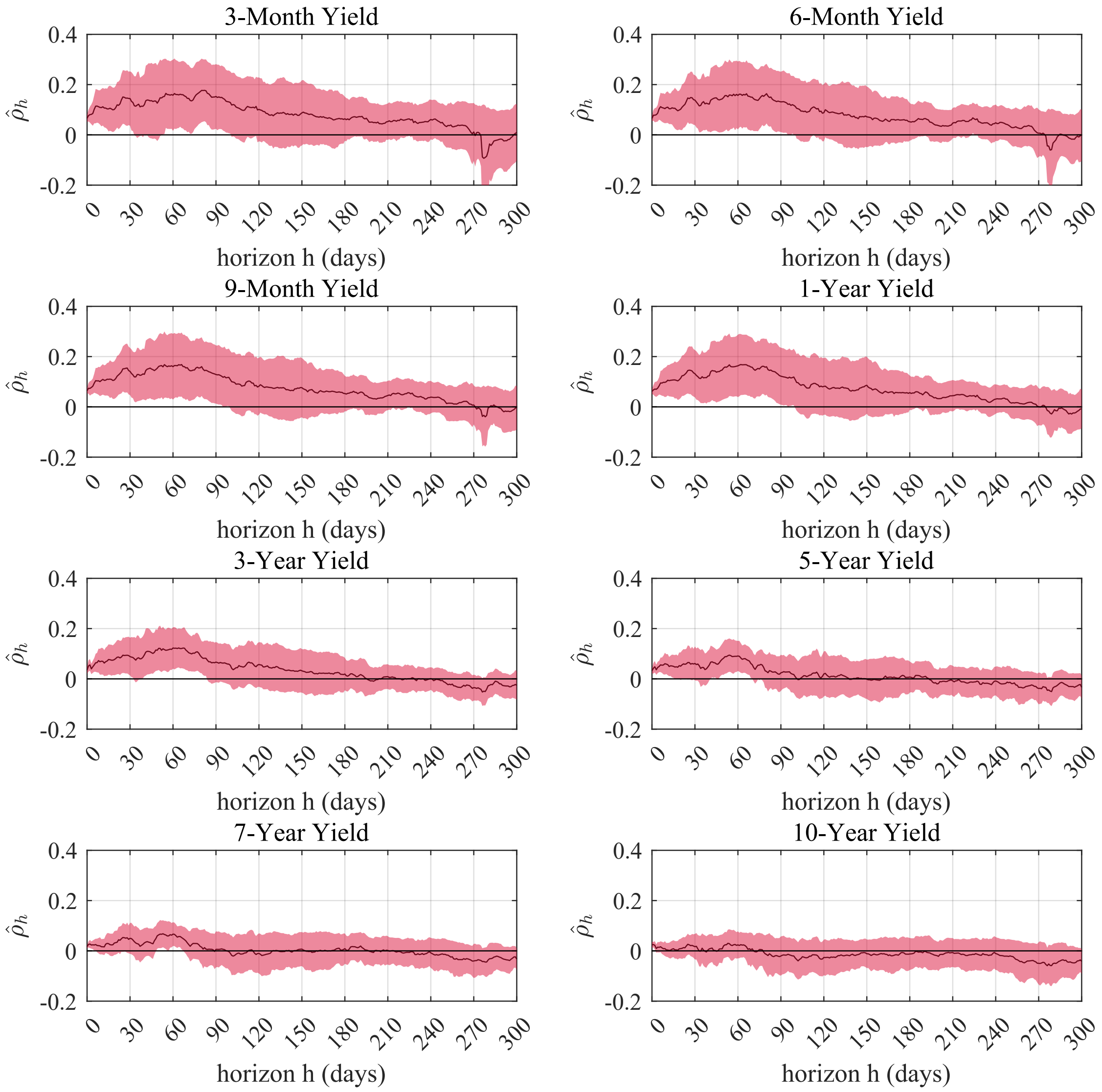

Figure 7: Impulse Responses of Treasury Bond Yields to Quantity-Target Loud-News Shocks

Note: This figure shows the impulse responses of Treasury bond yields to *Q-target L* shocks, identified from loud news in Q-announcements. The solid line plots the estimated coefficient $\hat{\rho}_h$ from the local projection $y_{t+h} = \upsilon_h + \rho_h Shock_t + \varphi_h y_{t-1} + \psi_h \tilde{F}_t + \epsilon_{t+h}$, where y_{t+h} is the yield at horizon h and $Shock_t$ is the *Q-target L* shock. The model controls for the lagged yield and a vector $\tilde{F}_t$ containing the other three identified policy shocks. The shaded area represents the 95% confidence interval based on HAC standard errors.

5.5 Dynamic Effects of Shocks on Money Market Rates

To complete our analysis of monetary policy transmission, we examine how the identified shocks propagate through China's money markets. As the PBoC gradually shifts toward a price-target-based policy framework, understanding how both quantity and price tools affect benchmark money market rates is essential. We employ the same local projection method used in the previous section to trace the dynamic responses of Shibor rates to all four policy

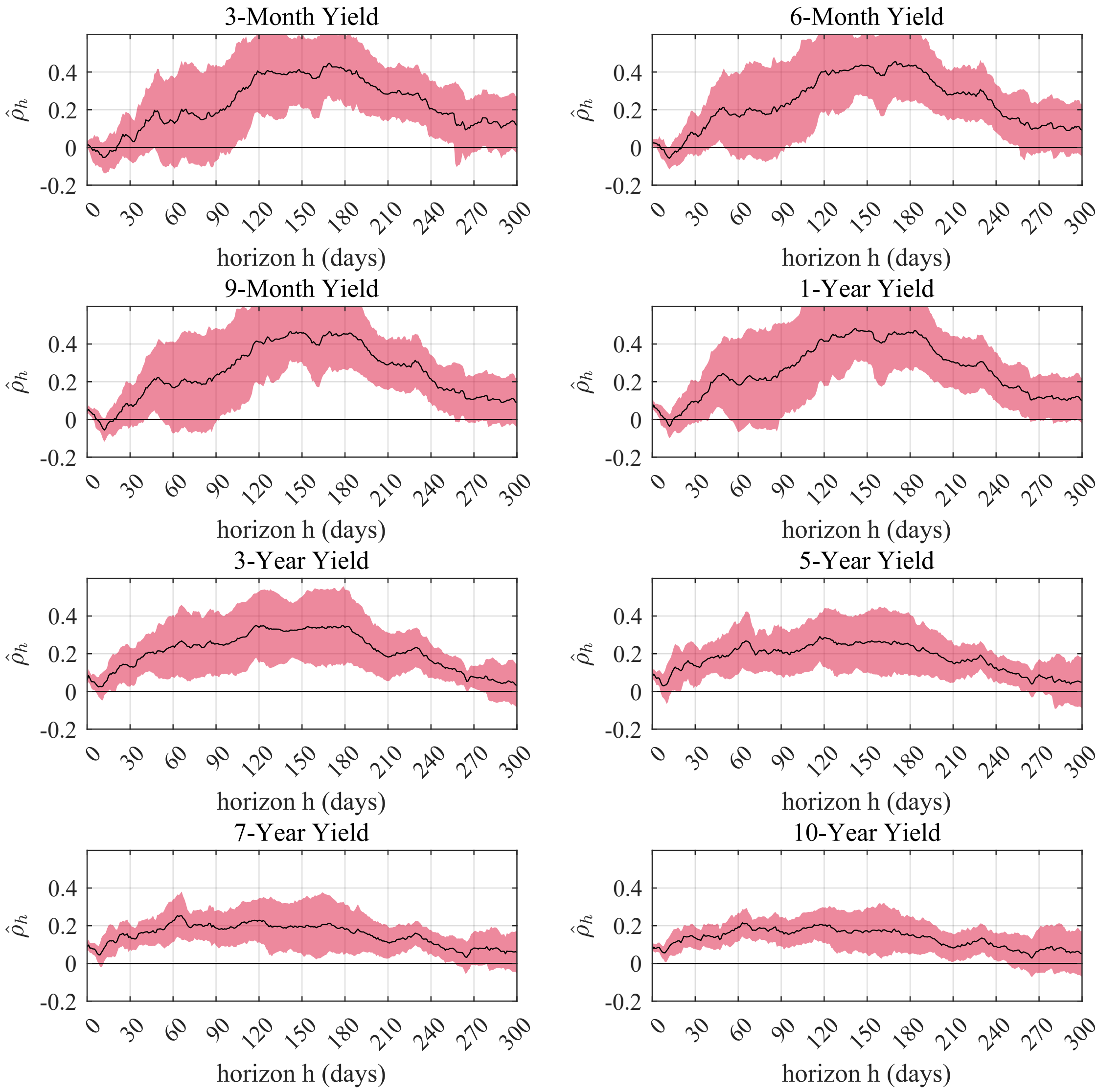

Figure 8: Impulse Responses of Treasury Bond Yields to Price-Target Loud-News Shocks

Note: This figure shows the impulse responses of Treasury bond yields to *P-target L* shocks, identified from loud news in P-announcements. The solid line plots the estimated coefficient $\hat{\rho}_h$ from the local projection $y_{t+h} = \upsilon_h + \rho_h Shock_t + \varphi_h y_{t-1} + \psi_h \tilde{F}_t + \epsilon_{t+h}$, where y_{t+h} is the yield at horizon h and $Shock_t$ is the *P-target L* shock. The model controls for the lagged yield and a vector $\tilde{F}_t$ containing the other three identified policy shocks. The shaded area represents the 95% confidence interval based on HAC standard errors.

shocks.

5.5.1 Responses to Loud-News Shocks

Q-target L shocks (Figure 11) transmit to Shibor rates with near-instantaneous effects, particularly for short-term maturities. The inherent volatility of short-term Shibor rates (as shown in Figure 3), however, leads to intermittent periods of statistical insignificance in the

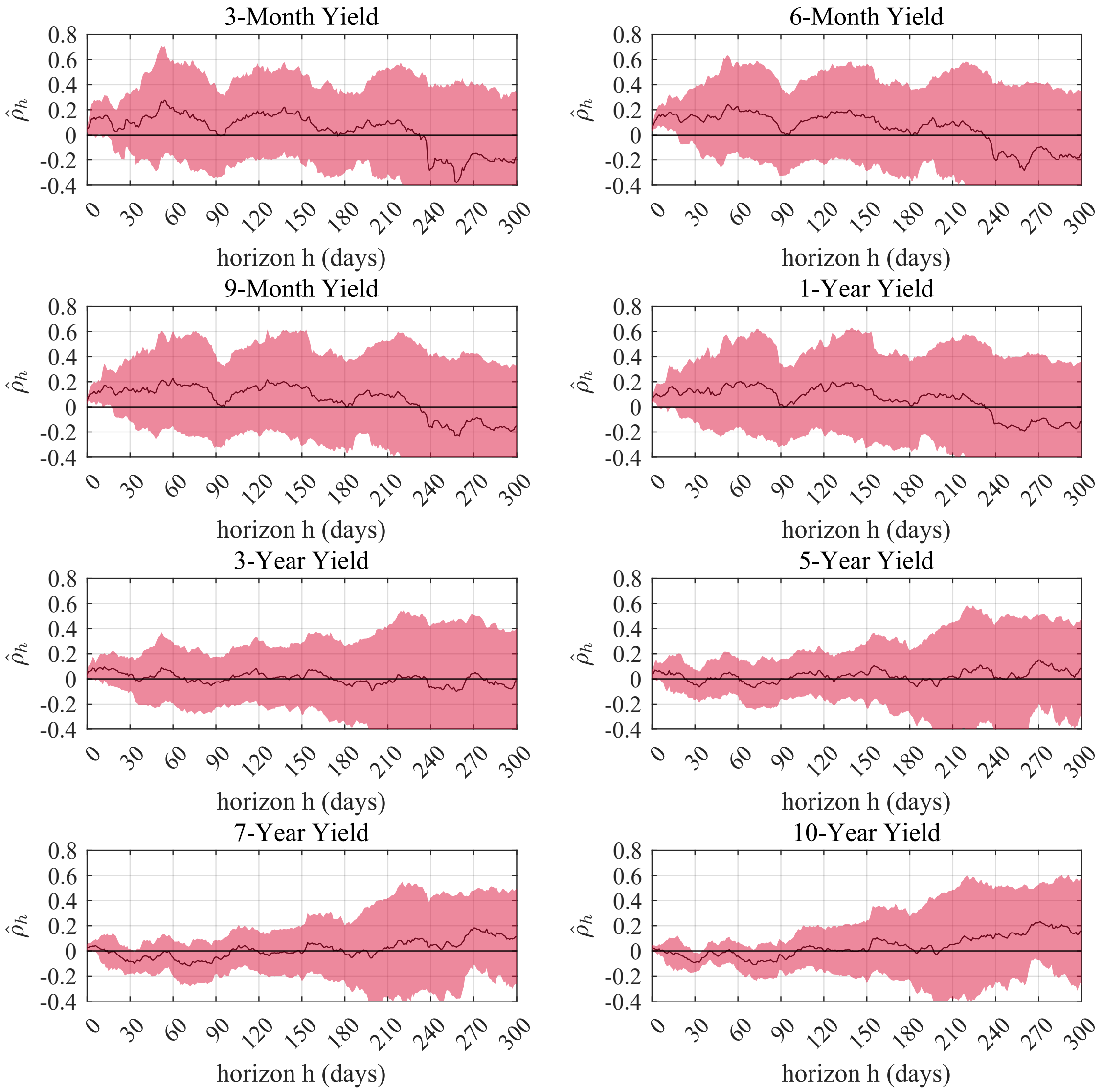

Figure 9: Impulse Responses of Treasury Bond Yields to Quantity-Target Silent-News Shocks

Note: This figure shows the impulse responses of Treasury bond yields to *Q-target S* shocks, identified from silent news in P-announcements. The solid line plots the estimated coefficient $\hat{\rho}_h$ from the local projection $y_{t+h} = \upsilon_h + \rho_h Shock_t + \varphi_h y_{t-1} + \psi_h \tilde{F}_t + \epsilon_{t+h}$, where y_{t+h} is the yield at horizon h and $Shock_t$ is the *Q-target S* shock. The model controls for the lagged yield and a vector $\tilde{F}_t$ containing the other three identified policy shocks. The shaded area represents the 95% confidence interval based on HAC standard errors.

response functions.[10]

P-target L shocks (Figure 12) produce a distinct time lag in the response of short-term Shibor rates, which become significant only after a delay. This pattern echoes the statistically insignificant immediate impact of P-target shocks on short-term Treasury yields reported in

[10]Similar unsmooth responses appear for other shocks as shown in the following figures. The pattern reflects the high sensitivity of short-term Shibor rates to transient interbank liquidity conditions, where liquidity shocks may periodically overwhelm the identifiable policy shock effect.

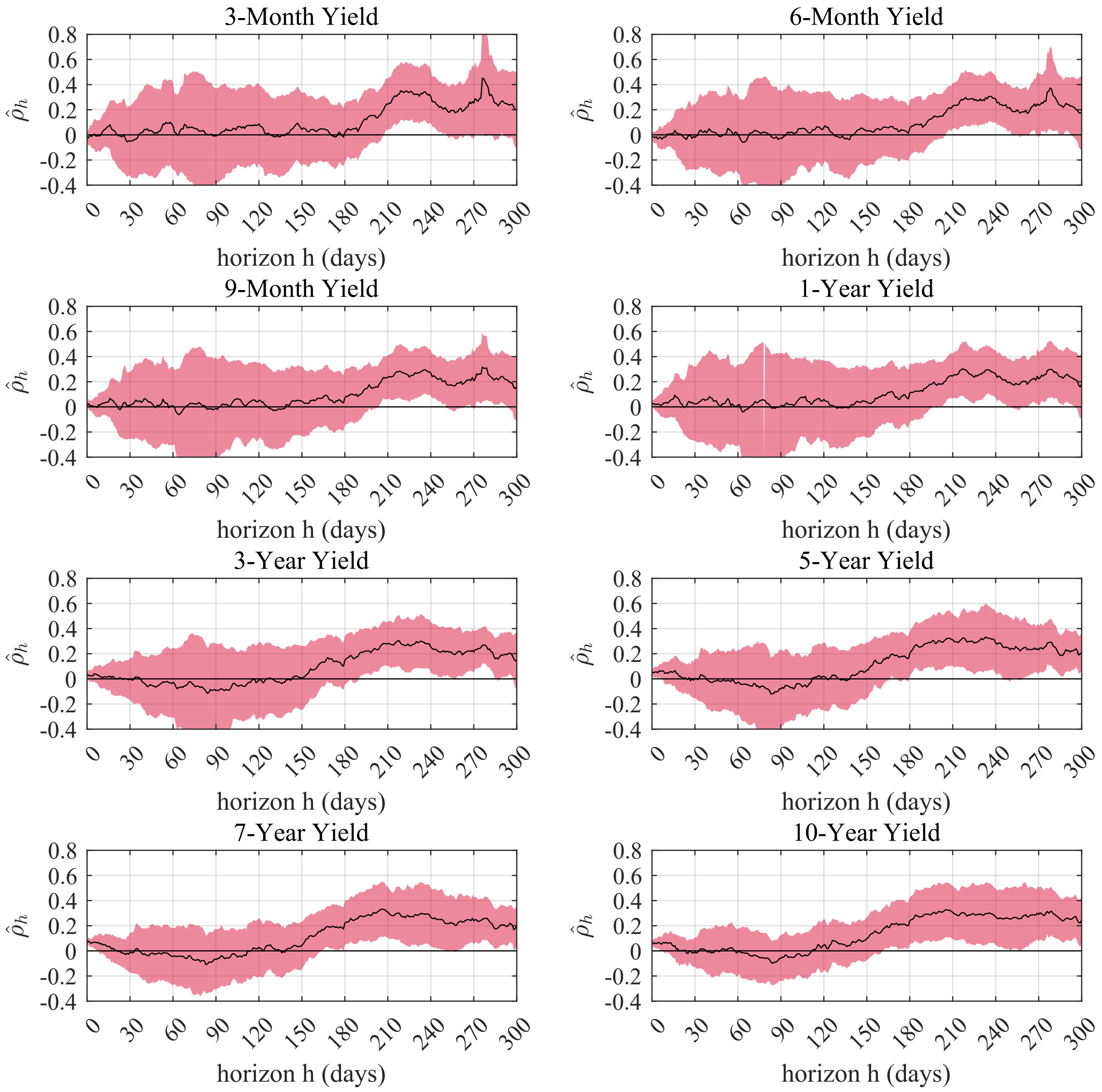

Figure 10: Impulse Responses of Treasury Bond Yields to Price-Target Silent-News Shocks

Note: This figure shows the impulse responses of Treasury bond yields to *P-target S* shocks, identified from silent news in Q-announcements. The solid line plots the estimated coefficient $\hat{\rho}_h$ from the local projection $y_{t+h} = \upsilon_h + \rho_h Shock_t + \varphi_h y_{t-1} + \psi_h \tilde{F}_t + \epsilon_{t+h}$, where y_{t+h} is the yield at horizon h and $Shock_t$ is the *P-target S* shock. The model controls for the lagged yield and a vector $\tilde{F}_t$ containing the other three identified policy shocks. The shaded area represents the 95% confidence interval based on HAC standard errors.

Table 2. As maturity increases, the lagged pattern diminishes, with 6-month, 9-month and 1-year Shibor rates showing significant immediate responses.

5.5.2 Responses to Silent-News Shocks

Q-target S shocks (Figure 13) elicit less pronounced responses from Shibor rates. Short-term rates show intermittent significant reactions after a delay, fluctuating between significance and insignificance, but generally become insignificant after about 210 trading days. This

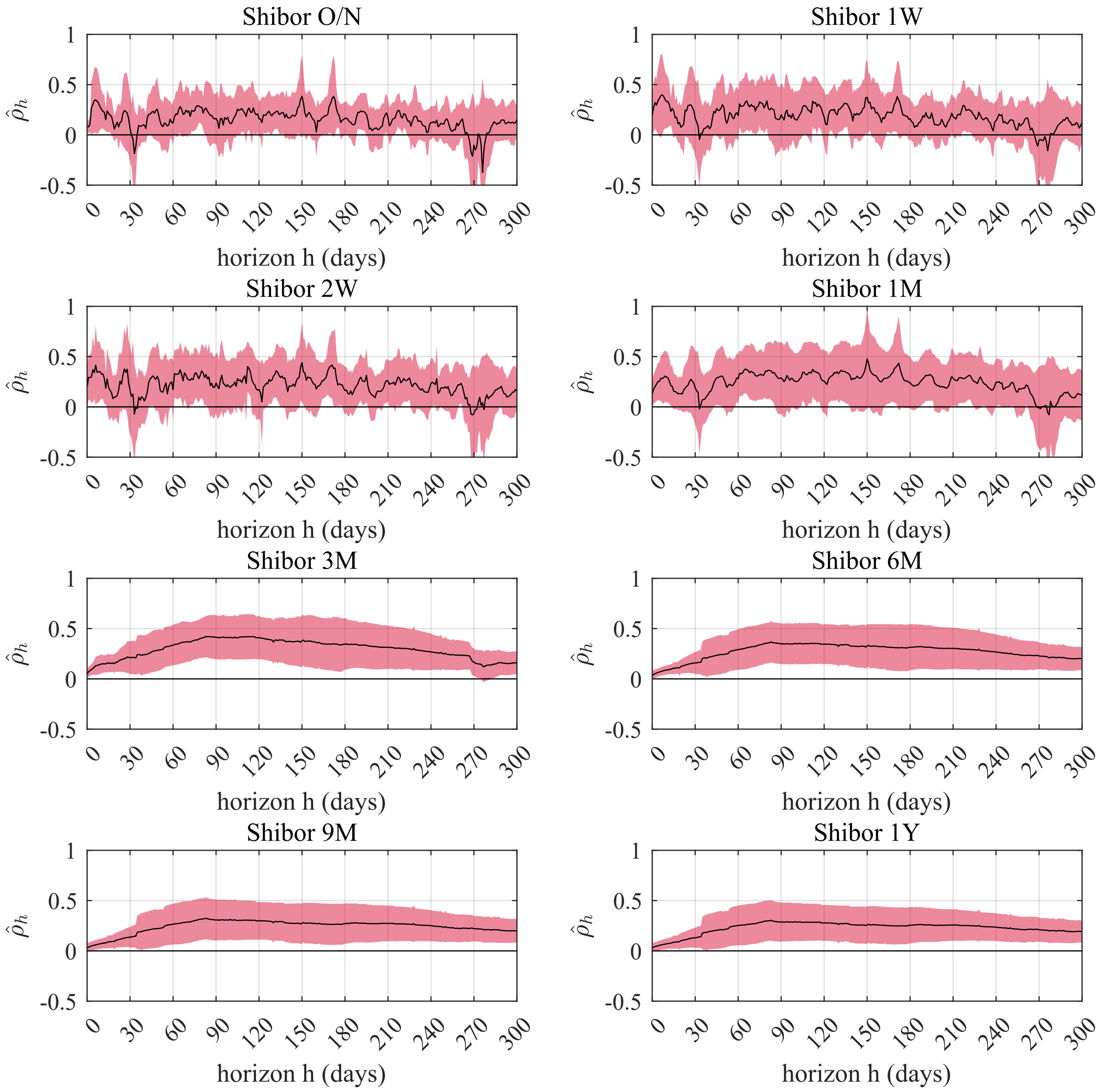

Figure 11: Impulse Responses of Shibor Rates to Quantity-Target Loud-News Shocks

Note: This figure shows the impulse responses of the Shibor rates to *Q-target L* shocks, identified from loud news in Q-announcements. The solid line plots the estimated coefficient $\hat{\rho}_h$ from the local projection $y_{t+h} = \upsilon_h + \rho_h Shock_t + \varphi_h y_{t-1} + \psi_h \tilde{F}_t + \epsilon_{t+h}$, where y_{t+h} is the Shibor rate at horizon h and $Shock_t$ is the *Q-target L* shock. The model controls for the lagged yield and a vector $\tilde{F}_t$ containing the other three identified policy shocks. The shaded area represents the 95% confidence interval based on HAC standard errors.

aligns with our earlier findings of their weaker heteroskedasticity and predictive power.

P-target S shocks (Figure 14) triggers significantly positive responses in Shibor rates with maturities exceeding 3 months after about 180 trading days. This lagged effect mirrors the response pattern of Treasury bond yields to the same shocks, reinforcing the economic meaning of silent news within Q-announcements.

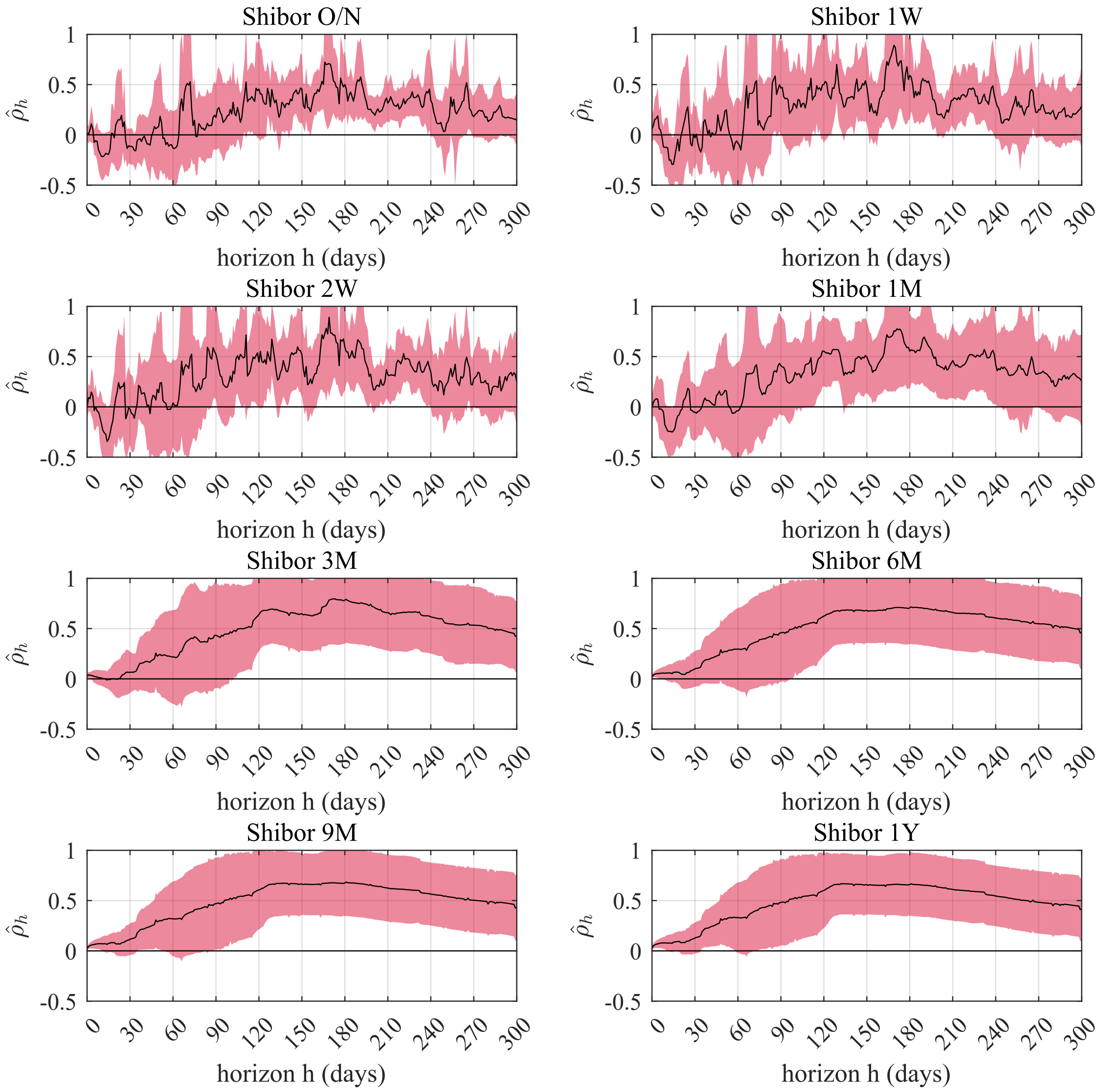

Figure 12: Impulse Responses of Shibor Rates to Price-Target Loud-News Shocks

Note: This figure shows the impulse responses of the Shibor rates to *P-target L* shocks, identified from loud news in P-announcements. The solid line plots the estimated coefficient $\hat{\rho}_h$ from the local projection $y_{t+h} = \upsilon_h + \rho_h Shock_t + \varphi_h y_{t-1} + \psi_h \tilde{F}_t + \epsilon_{t+h}$, where y_{t+h} is the Shibor rate at horizon h and $Shock_t$ is the *P-target L* shock. The model controls for the lagged yield and a vector $\tilde{F}_t$ containing the other three identified policy shocks. The shaded area represents the 95% confidence interval based on HAC standard errors.

5.5.3 Implications for China's Evolving Policy Framework

The impulse response evidence demonstrates that the PBoC's monetary policy announcements transmit to money market rates through multiple and parallel channels—consistent with the mechanism observed for Treasury bond yields. Specifically, explicit quantity-target shocks exert an immediate impact on money markets, whereas explicit price-target shocks affect short-term money-market rates with a discernible lag. This finding corroborates our

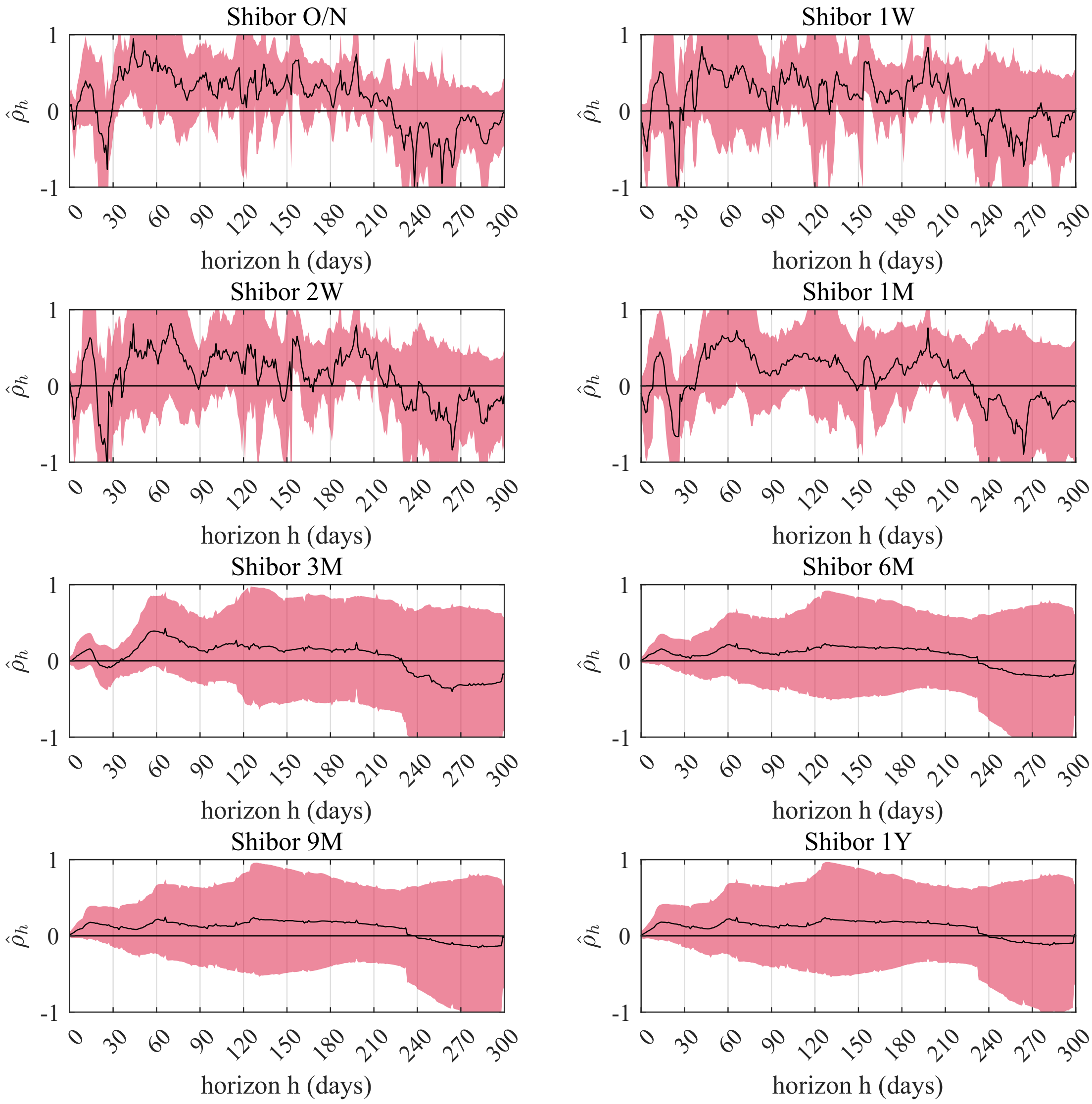

Figure 13: Impulse Responses of Shibor Rates to Quantity-Target Silent-News Shocks

Note: This figure shows the impulse responses of the Shibor rates to *Q-target S* shocks, identified from loud news in P-announcements. The solid line plots the estimated coefficient $\hat{\rho}_h$ from the local projection $y_{t+h} = \upsilon_h + \rho_h Shock_t + \varphi_h y_{t-1} + \psi_h \tilde{F}_t + \epsilon_{t+h}$, where y_{t+h} is the Shibor rate at horizon h and $Shock_t$ is the *Q-target S* shock. The model controls for the lagged yield and a vector $\tilde{F}_t$ containing the other three identified policy shocks. The shaded area represents the 95% confidence interval based on HAC standard errors.

earlier argument regarding the delayed transmission of medium- to long-term price-target adjustments to short-term rates. Meanwhile, implicitly signaled price-target shocks also show lagged effects on money markets, operating through a forward-looking signaling channel that conveys information about prospective policy adjustments.

These results offer important insights for China's evolving monetary policy framework. Historically, unlike developed economies that primarily steer longer-term yields by adjusting short-term policy rates through market-based transmission, China has often influenced

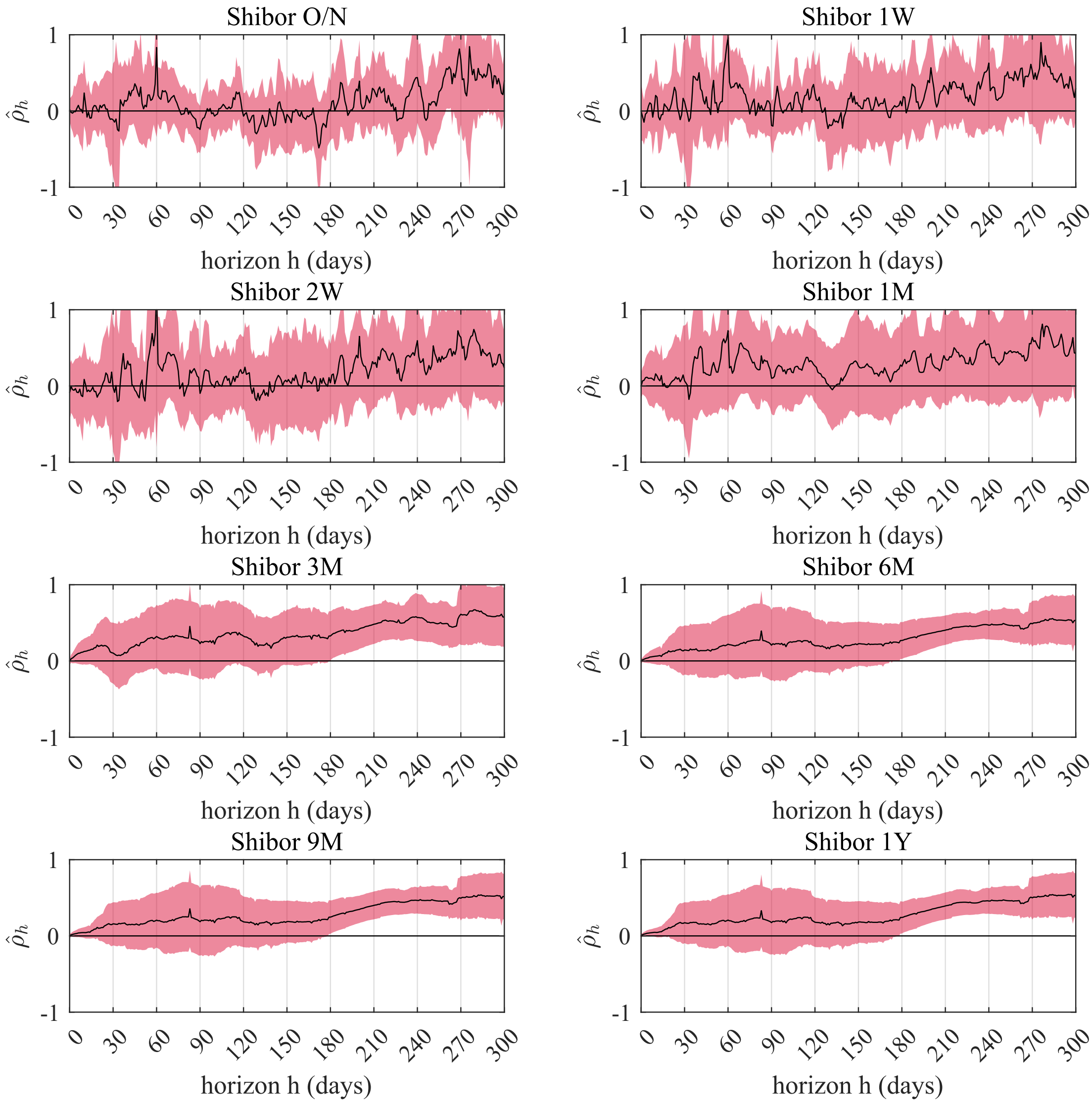

Figure 14: Impulse Responses of Shibor Rates to Price-Target Silent-News Shocks

Note: This figure shows the impulse responses of the Shibor rates to *P-target S* shocks, identified from loud news in Q-announcements. The solid line plots the estimated coefficient $\hat{\rho}_h$ from the local projection $y_{t+h} = \upsilon_h + \rho_h Shock_t + \varphi_h y_{t-1} + \psi_h \tilde{F}_t + \epsilon_{t+h}$, where y_{t+h} is the Shibor rate at horizon h and $Shock_t$ is the *P-target S* shock. The model controls for the lagged yield and a vector $\tilde{F}_t$ containing the other three identified policy shocks. The shaded area represents the 95% confidence interval based on HAC standard errors.

lending costs of commercial bank by directly setting medium- to long-term interest-rate targets. While this administrative approach can affect real-economy financing conditions more swiftly, it carries the risk of policy overshooting/undershooting and, as shown here, exhibits a transmission lag to short-term money market. These factors have rendered the central bank cautious in adjusting medium- to long-term price targets, contributing to a heavier reliance on quantitative tools—a practice that has, in turn, fostered market demand for clearer price signals.

Driven by these limitations and the broader goal of interest rate liberalization, it is imperative for the PBoC to transition toward a framework that anchors short-term rates to steer longer-term yields via market mechanisms. This logic underpins the PBoC's recent shift toward using the 7-day reverse repo rate as its key policy benchmark. Under the continuing quantity-price dual-tool framework, policymakers must deliberately account for the inherent interest-rate signals embedded in quantitative operations to ensure they reinforce, rather than contradict, the intended policy stance.

6 Conclusions

This paper develops a novel framework for analyzing China's unique dual-target monetary policy. Recognizing that PBoC announcements under its coordinated quantity-price framework contain both explicit (loud) and implicit (silent) news, we move beyond the conventional single-shock paradigm to identify and economically label the dual shocks embedded within these announcements.

Our primary methodological contribution is an ordered-heteroskedasticity identification strategy. This approach refines the use of heteroskedasticity from a tool that merely detects the presence of shocks to one that systematically classifies them. By imposing an intuitive variance ordering, where a given target shock exhibits higher volatility when it is the loud focus of an announcement than when it is silently signaled, we achieve two key outcomes: we disentangle the two unobservable shocks without relying on observable target surprises or restrictive theory-based assumptions, and we directly solve the labeling problem by assigning clear economic identities as quantity-target versus price-target shocks.

Empirically, our dual-shock model significantly outperforms the traditional single-shock specification in explaining yield innovations across the term structure. We uncover distinct transmission channels: quantity-target shocks exert a stronger influence on short-term Treasury yields, while the impact of price-target shocks increases with bond maturity. Crucially, silent news proves economically potent. Implicit price-target shocks within quantity announcements provide powerful forward guidance, significantly predicting the PBoC's future price-target adjustments. Moreover, both explicit and implicit target shocks trigger significant and persistent dynamic responses in Treasury bond yields and money market rates (Shibor), with silent price news containing predictive information about substantial future interest-rate movements.

These findings carry important implications. For the PBoC, this research illuminates a potent indirect transmission channel: quantitative adjustments systematically shape market expectations for future price settings, thereby influencing money market rates through both direct liquidity and indirect signaling effects. A deeper understanding of this mechanism can help refine the central bank's communication strategy and improve the coordination of its dual-tool framework. For global investors and economists, our study offers a more nuanced and accurate toolkit for decoding the content and market effects of China's monetary policy communications.

Looking ahead, several promising research avenues emerge. First, the identified quantity- and price-target shocks can be integrated into broader macroeconomic models to trace their differential impacts on the real economy and financial stability, thereby deepening our understanding of China's complete monetary transmission mechanism. Second, the ordered-heteroskedasticity framework is highly generalizable. It can be adapted to identify policy shocks in other economies that employ multiple tools, or to analyze other high-frequency financial events where multiple unobservable shocks coexist and conventional identification methods falter. A key challenge for future work will be to extend the logic of ordered heteroskedasticity into other multifactor identification settings with time-varying volatility, thereby equipping them to economically label the identified shocks.

Acknowledgements

This research is supported by the National Natural Science Foundation of China (Grant Nos. 72103068, 72273118, 72203237, 71988101).

References

Altavilla, C., L. Brugnolini, R. S. Gürkaynak, R. Motto, and G. Ragusa (2019). Measuring euro area monetary policy. *Journal of Monetary Economics 108*, 162–179.

Andrade, P. and F. Ferroni (2021). Delphic and odyssean monetary policy shocks: Evidence from the euro area. *Journal of Monetary Economics 117*, 816–832.

Brand, C., D. Buncic, and J. Turunen (2010). The impact of ECB monetary policy decisions and communication on the yield curve. *Journal of the European Economic Association 8*(6), 1266–1298.

Bu, C., J. Rogers, and W. Wu (2021). A unified measure of Fed monetary policy shocks. *Journal of Monetary Economics 118*, 331–349.

Campbell, J. R., C. L. Evans, J. D. Fisher, A. Justiniano, C. W. Calomiris, and M. Woodford (2012). Macroeconomic effects of federal reserve forward guidance [with comments and discussion]. *Brookings papers on economic activity*, 1–80.

Cieslak, A. and A. Schrimpf (2019). Non-monetary news in central bank communication. *Journal of International Economics 118*, 293–315.

Clark, P. K. (1973). A subordinated stochastic process model with finite variance for speculative prices. *Econometrica 41*(1), 135–155.

Cook, T. and T. Hahn (1989). The effect of changes in the federal funds rate target on market interest rates in the 1970s. *Journal of Monetary Economics 24*(3), 331–351.

Das, S. and W. Song (2023). Monetary policy transmission and policy coordination in China. *China Economic Review 82*, 102032.

Gertler, M. and P. Karadi (2015, January). Monetary policy surprises, credit costs, and economic activity. *American Economic Journal: Macroeconomics 7*(1), 44–76.

Ghysels, E., A. C. Harvey, and E. Renault (1996). 5 stochastic volatility. In *Statistical Methods in Finance*, Volume 14 of *Handbook of Statistics*, pp. 119–191. Elsevier.

Gürkaynak, R. S., B. Kisacikoglu, and J. H. Wright (2020, December). Missing events in event studies: Identifying the effects of partially measured news surprises. *American Economic Review 110*(12), 3871–3912.

Gürkaynak, R. S., B. Sack, and E. T. Swansonc (2005). Do actions speak louder than words? the response of asset prices to monetary policy actions and statements. *International Journal of Central Banking 1*, 55–93.

Hanson, S. G., A. Shleifer, J. C. Stein, and R. W. Vishny (2015). Banks as patient fixed-income investors. *Journal of Financial Economics 117*(3), 449–469.

He, J. J., C. D. Jia, K. Li, and W. Wu (2023). A high-frequency measure of Chinese monetary policy shocks. *Available at SSRN 4599848*.

Jarociński, M. (2024). Estimating the Fed's unconventional policy shocks. *Journal of Monetary Economics 144*, 103548.

Jarociński, M. and P. Karadi (2020, April). Deconstructing monetary policy surprises—the role of information shocks. *American Economic Journal: Macroeconomics 12*(2), 1–43.

Kaminska, I., H. Mumtaz, and R. Šustek (2021). Monetary policy surprises and their transmission through term premia and expected interest rates. *Journal of Monetary Economics 124*, 48–65.

Kuttner, K. N. (2001). Monetary policy surprises and interest rates: Evidence from the Fed funds futures market. *Journal of Monetary Economics 47*(3), 523–544.

Lanne, M., H. Lütkepohl, and K. Maciejowska (2010). Structural vector autoregressions with markov switching. *Journal of Economic Dynamics and Control 34*(2), 121–131.

Lewis, D. J. (2021, May). Identifying shocks via time-varying volatility. *The Review of Economic Studies 88*(6), 3086–3124.

Lewis, D. J. (2025, 07). Announcement-specific decompositions of unconventional monetary policy shocks and their effects. *The Review of Economics and Statistics 107*(4), 1086–1103.

Li, J., V. Todorov, and Q. Zhang (2024, 03). Testing the dimensionality of policy shocks. *The Review of Economics and Statistics 106*(2), 470–482.

Lin, M. and L. Niu (2021). Echo over the great wall: Spillover effects of QE announcements on Chinese yield curve. *Journal of International Money and Finance 111*, 102294.

Lu, D., H. Tang, and C. Zhang (2023). China's monetary policy surprises and corporate real investment. *China Economic Review 77*, 101893.

Lunsford, K. G. (2020, September). Policy language and information effects in the early days of Federal Reserve forward guidance. *American Economic Review 110*(9), 2899–2934.

Nakamura, E. and J. Steinsson (2018). High-frequency identification of monetary non-neutrality: the information effect. *The Quarterly Journal of Economics 133*(3), 1283–1330.

Politis, D. N. and J. P. Romano (1994). The stationary bootstrap. *Journal of the American Statistical Association 89*(428), 1303–1313.

Rigobon, R. (2003). Identification through heteroskedasticity. *Review of Economics and Statistics 85*(4), 777–792.

Rigobon, R. and B. Sack (2004). The impact of monetary policy on asset prices. *Journal of Monetary Economics 51*(8), 1553–1575.

Stock, J. H. and M. W. Watson (2018, 5). Identification and estimation of dynamic causal effects in macroeconomics using external instruments. *The Economic Journal 128*, 917–948.

Swanson, E. (2021). Measuring the effects of Federal Reserve forward guidance and asset purchases on financial markets. *Journal of Monetary Economics 118*, 32–53.

Swanson, E. and V. Jayawickrema (2024). Speeches by the Fed chair are more important than FOMC announcements: An improved high-frequency measure of us monetary policy shocks. *Unpublished Manuscript*.

Vayanos, D. and J.-L. Vila (2021). A preferred-habitat model of the term structure of interest rates. *Econometrica 89*(1), 77–112.

Wright, J. H. (2012). What does monetary policy do to long-term interest rates at the zero lower bound? *The Economic Journal 122*(564), 447 – 466.

A Appendix

A.1 Examples of Monetary Announcements

Figure A.1: An Example of a PBoC Quantity Announcement

Note: This figure reproduces the official announcement by the People's Bank of China (PBoC) dated June 7, 2008 (available at: http://www.pbc.gov.cn/zhengcehuobisi/125207/125213/125434/125798/2835308/index.html). This announcement serves as a characteristic example of a quantity-target-based announcement (Q-announcement) within the PBoC's dual-tool framework.

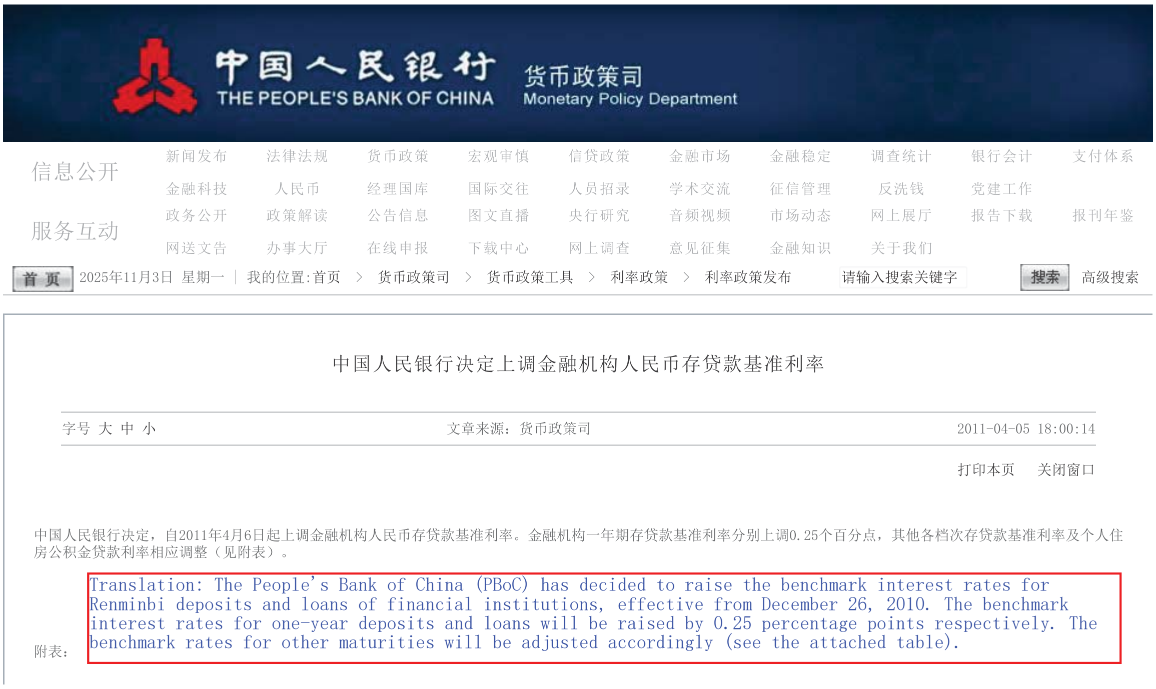

中国人民银行 THE PEOPLE'S BANK OF CHINA 货币政策司 Monetary Policy Department

信息公开 新闻发布 法律法规 货币政策 宏观审慎 信贷政策 金融市场 金融稳定 调查统计 银行会计 支付体系 金融科技 人民币 经理国库 国际交往 人员招录 学术交流 征信管理 反洗钱 党建工作

服务互动 政务公开 政策解读 公告信息 图文直播 央行研究 音频视频 市场动态 网上展厅 报告下载 报刊年鉴 网送文告 办事大厅 在线申报 下载中心 网上调查 意见征集 金融知识 关于我们

首页 2025年11月3日 星期一 | 我的位置:首页 > 货币政策司 > 货币政策工具 > 利率政策 > 利率政策发布 请输入搜索关键字 搜索 高级搜索

中国人民银行决定上调金融机构人民币存贷款基准利率

字号 大 中 小 文章来源：货币政策司 2011-04-05 18:00:14

打印本页 关闭窗口

中国人民银行决定，自2011年4月6日起上调金融机构人民币存贷款基准利率。金融机构一年期存贷款基准利率分别上调0.25个百分点，其他各档次存贷款基准利率及个人住房公积金贷款利率相应调整（见附表）。

Translation: The People's Bank of China (PBoC) has decided to raise the benchmark interest rates for Renminbi deposits and loans of financial institutions, effective from December 26, 2010. The benchmark interest rates for one-year deposits and loans will be raised by 0.25 percentage points respectively. The benchmark rates for other maturities will be adjusted accordingly (see the attached table).

附表：

Figure A.2: An Example of a PBoC Price Announcement

Note: This figure reproduces the official announcement by the People's Bank of China (PBoC) dated April 5, 2011 (available at: http://www.pbc.gov.cn/zhengcehuobisi/125207/125213/125440/125835/2876411/index.html). This announcement serves as a characteristic example of a price-target-based announcement (P-announcement) within the PBoC's dual-tool framework.

A.2 Monetary Policy Events

Table A.1: Historical Monetary Policy Adjustments in China (2006-2022)

No.	Date	Time	RRR(%)	BLDR (%)	MLF rate (%)
1	2006/11/3	18:15:00	+0.5	–	–
2	2007/1/5	17:14:00	+0.5	–	–
3	2007/2/16	16:00:00	+0.5	–	–
4	2007/3/17	17:01:00	–	+0.27	–
5	2007/4/5	17:19:00	+0.5	–	–
6	2007/4/29	11:30:00	+0.5	–	–
7	2007/5/18	18:38:00	+0.5	+0.18	–
8	2007/7/20	17:25:00	–	+0.27	–
9	2007/7/30	17:39:00	+0.5	–	–
10	2007/8/21	18:30:00	–	+0.18	–
11	2007/9/6	18:00:00	+0.5	–	–
12	2007/9/14	17:34:00	–	+0.27	–
13	2007/10/13	15:00:00	+0.5	–	–
14	2007/11/10	17:00:00	+0.5	–	–
15	2007/12/8	16:00:00	+1.0	–	–
16	2007/12/20	18:00:00	–	+0.18	–
17	2008/1/16	18:00:00	+0.5	–	–
18	2008/3/18	18:00:00	+0.5	–	–
19	2008/4/16	17:00:00	+0.5	–	–
20	2008/5/12	16:20:00	+0.5	–	–
21	2008/6/7	18:07:00	+0.5	–	–
22	2008/9/15	17:01:00	+0.5	-0.27	–
23	2008/10/8	18:58:00	-0.5	-0.27	–
24	2008/10/29	19:00:00	–	-0.27	–
25	2008/11/26	16:45:00	-1.0	-1.08	–
26	2008/12/22	18:32:00	-0.5	-0.27	–
27	2010/1/12	19:00:00	+0.5	–	–
28	2010/2/12	18:00:00	+0.5	–	–
29	2010/5/2	18:43:27	+0.5	–	–
30	2010/10/19	18:59:36	–	+0.25	–
31	2010/11/10	18:45:00	+0.5	–	–
32	2010/11/19	17:59:46	+0.5	–	–
33	2010/12/10	18:00:01	+0.5	–	–

Continued on next page

(Continued from previous page)					
No.	**Date**	**Time**	**RRR (%)**	**BLDR (%)**	**MLF rate(%)**
34	2010/12/25	17:35:21	–	+0.25	–
35	2011/1/14	17:55:26	+0.5	–	–
36	2011/2/8	18:30:30	–	+0.25	–
37	2011/2/18	18:02:18	+0.5	–	–
38	2011/3/18	18:20:56	+0.5	–	–
39	2011/4/5	18:00:14	–	+0.25	–
40	2011/4/17	17:02:15	+0.5	–	–
41	2011/5/12	18:30:02	+0.5	–	–
42	2011/6/14	15:18:25	+0.5	–	–
43	2011/7/6	18:32:12	–	+0.25	–
44	2011/11/30	19:03:42	-0.5	–	–
45	2012/2/18	20:00:00	-0.5	–	–
46	2012/5/12	19:00:00	-0.5	–	–
47	2012/6/7	19:00:00	–	-0.25	–
48	2012/7/5	19:00:00	–	-0.31	–
49	2014/11/21	18:30:15	–	-0.40	–
50	2015/2/4	18:21:17	-0.5	–	–
51	2015/2/28	17:54:59	–	-0.25	–
52	2015/4/19	17:01:07	-1.0	–	–
53	2015/5/10	17:00:54	–	-0.25	–
54	2015/6/27	16:55:24	-0.5	-0.25	–
55	2015/8/25	18:15:34	-0.5	-0.25	–
56	2015/10/23	19:17:52	-0.5	-0.25	–
57	2016/2/29	18:00:00	-0.5	–	–
58	2018/4/17	18:26:32	-1.0	–	–
59	2018/6/24	17:02:18	-0.5	–	–
60	2018/10/7	11:49:46	-1.0	–	–
61	2019/1/4	17:20:40	-1.0	–	–
62	2019/9/6	17:22:05	-0.5	–	–
63	2019/11/5	10:35:00	–	–	-0.05
64	2020/1/1	15:07:56	-0.5	–	–
65	2020/2/17	10:25:00	–	–	-0.10
66	2020/4/15	09:48:00	–	–	-0.20
67	2021/7/9	17:11:24	-0.5	–	–
68	2021/12/6	17:00:00	-0.5	–	–

Continued on next page

(Continued from previous page)					
No.	**Date**	**Time**	**RRR (%)**	**BLDR (%)**	**MLF rate(%)**
69	2022/1/17	09:20:00	–	–	-0.10
70	2022/4/15	18:14:39	-0.25	–	–
71	2022/8/15	09:20:00	–	–	-0.10
72	2022/11/25	17:41:00	-0.25	–	–

Notes:

1. **RRR**: Reserve Requirement Ratio. The PBoC applies differentiated reserve requirement ratios to large deposit-taking financial institutions and small-to-medium deposit-taking financial institutions. For brevity, only adjustments applicable to large financial institutions are presented here.
2. **BLDR**: Benchmark Lending and Deposit Rates. The PBoC sets benchmark rates for deposits and loans across multiple terms. Deposit rates cover demand deposits and various time deposit tenors (e.g., 3-month, 6-month, 1-year, 2-year, 3-year, and 5-year). Loan rates are segmented by maturity intervals (e.g., 6-months, 6-month to 1-year, 1-year to 3-year, 3-year to 5-year, and over 5-year). Adjustments to these rates occur periodically, with changes often varying by term. Notably, in 2014, the loan rate structure was simplified into three main categories, and the 5-year deposit benchmark was discontinued. The table lists the 6-month to 1-year loan rate (under 1-year after Nov 2014) due to space limitations.
3. **MLF rate**: 1-year Medium-term Lending Facility rate. The MLF was initially introduced with rates for multiple tenors, but the PBoC has since shifted to adjusting only the 1-year rate as the primary policy benchmark. MLF rate adjustments prior to August 17, 2019, are excluded because, as discussed in Section 4.1.2, the MLF rate became the de facto medium-term policy anchor only after the LPR reform on that date.
4. All values represent percentage-point changes; a plus sign (+) indicates an increase, and a minus sign (-) indicates a decrease.
5. "–" indicates no adjustment for that instrument on the date.
6. Shaded rows indicate simultaneous adjustments to both RRR and benchmark interest rates.
7. Data source: Announcements regarding the RRR and BLDR were obtained from the official website of the PBoC, while MLF rate announcements were sourced from the National Interbank Funding Center.